

Implication of a vanishing element in the 3 + 1 scenarioMonojit Ghosh,^{1,*} Srubabati Goswami,^{1,†} Shivani Gupta,^{2,‡} and C. S. Kim^{2,§}¹*Physical Research Laboratory, Navrangpura, Ahmedabad 380 009, India*²*Department of Physics and IPAP, Yonsei University, Seoul 120-479, Korea*

(Received 7 May 2013; published 19 August 2013)

In this paper we study the phenomenological implications of the one-zero textures of low energy neutrino mass matrices in the presence of a sterile neutrino. We consider the 3 + 1 scheme and use the results from a global fit for short baseline neutrino oscillation data, which provides the bounds on the three additional mixing angles. We find that the mass matrix elements $m_{\alpha\beta}$ ($\alpha, \beta = e, \mu, \tau$) involving only the active states can assume vanishing values in the allowed parameter space for all of the mass spectrum. Among the mass matrix elements connecting the active and sterile states, $m_{e s}$ and $m_{\mu s}$ can become small only for the quasidegenerate neutrinos. The element $m_{\tau s}$, on the other hand, can vanish even for lower values of masses since the 3–4 mixing angle only has an upper bound from current data. The mass matrix element ($m_{s s}$) involving only the sterile state stays $\sim \mathcal{O}(1)$ eV in the whole parameter region. We study the possible correlations between the sterile mixing angles and the Majorana phases to give a zero element in the mass matrix.

DOI: [10.1103/PhysRevD.88.033009](https://doi.org/10.1103/PhysRevD.88.033009)

PACS numbers: 14.60.Pq, 14.60.Lm, 13.15.+g

I. INTRODUCTION

Light sterile neutrinos were invoked to explain the results of the LSND experiment, which reported oscillation events in the $\bar{\nu}_\mu - \bar{\nu}_e$ mode corresponding to a mass squared difference $\sim eV^2$ [1]. Adding one sterile neutrino to the standard three-generation framework gives rise to two possible mass spectra—the 2 + 2 in which two pairs of mass states are separated by a difference $\sim eV^2$, and the 3 + 1 in which a single predominantly sterile state differs by $\sim eV^2$ from the three active states [2]. Subsequently, the 2 + 2 schemes were found to be incompatible with the solar and atmospheric neutrino data [3]. The MiniBoone experiment was designed to test this, and its antineutrino data confirmed the LSND anomaly [4]. Both 3 + 1 and 3 + 2 sterile neutrino schemes have been considered to explain these results [5–7]. Such global fits aim to explain the nonobservance of eV^2 oscillations in the disappearance channel in other short baseline experiments, as well as the reported evidence in LSND/MiniBoone experiments. The relevant probabilities for the 3 + 1 case are governed by a single mass squared difference and hence are independent of the CP phase. In the 3 + 2 scheme, dependence on CP phase comes into play and one gets a slightly better fit.

Other evidence in support of sterile neutrinos includes the reactor and the Ga anomaly. The first one refers to the deficit in the measured electron antineutrino flux in several experiments where the theoretical predictions of reactor neutrino fluxes were reevaluated [8]. The second one

implies a shortfall of electron neutrinos observed in the solar neutrino detectors GALLEX and SAGE using radioactive sources [9]. Both of these can be explained by adding light sub-eV sterile neutrinos in the three-generation framework.

There has also been some hint in favor of sterile neutrinos from cosmological observations of a “dark radiation” which is weakly interacting and relativistic. Attributing this to sterile neutrinos, one gets the bound on the number of neutrinos as $N_{\text{eff}} = 4.34 \pm 0.87$ at 68% C.L. [10]. The Planck satellite experiment, which has very recently declared its first results [11], on the other hand, gives $N_{\text{eff}} = 3.30 \pm 0.27$ at 68% C.L., which allows for an extra sterile neutrino at 95% C.L., although its mixing with active species can be very tightly constrained [12] within the framework of standard cosmology. Thus, the sterile neutrinos continue to be intriguing, and many new experiments are planned to test this [13].

Theoretically, sterile neutrinos are naturally included in the type-I seesaw model [14]. But their mass scale is usually very high to account for the small mass of the neutrinos. Light sub-eV sterile neutrinos, as suggested by the data, can arise in many models [13].

Irrespective of the mechanism for the generation of neutrino masses, the low energy Majorana mass matrix, in the presence of an extra sterile neutrino, will be of dimension 4×4 with ten independent entries and is given as

$$M_\nu = V^* M_\nu^{\text{diag}} V^\dagger, \quad (1)$$

where $M_\nu^{\text{diag}} = \text{Diag}(m_1, m_2, m_3, m_4)$ and V denotes the leptonic mixing matrix in the basis where the charged lepton mass matrix is diagonal. One of the important aims in the study of neutrino physics is to explore the structure of the neutrino mass matrices. At the fundamental level these

*monojit@prl.res.in

†sruba@prl.res.in

‡shivani@cskim.yonsei.ac.kr

§Corresponding author.

cskim@yonsei.ac.kr

are governed by Yukawa couplings, which are essentially free parameters in most models. These couplings motivated the study of texture zeros, which means one or more elements are relatively small compared to the others. Texture zeros in the low energy mass matrices in the context of three generations have been extensively explored, both in the quark and lepton sectors [15,16]. Such studies help us to understand the underlying parameter space and the nature of the mass spectrum involved and often predict correlations between various parameters which can be experimentally tested. For the three-generation scenario it is well known that the number of maximum texture zeros in a low energy mass matrix is two [15]. In the context of the four-neutrino case, however, more than two zeros may be allowed [17]. Two-zero textures of sterile neutrinos have been studied recently in [17], and three zero cases have been considered in [18]. In this paper we concentrate on the textures where one of the mass matrix elements is vanishing. For the 4×4 symmetric mass matrix there are a total of 10 different cases that need to be investigated. We study the implications of one-zero textures and the possible correlations between the parameters. We also compare our results with the one-zero textures for three active neutrinos [19,20].

The plan of the paper is as follows. In Sec. II we discuss the possible mass spectra and the mixing matrix in the 3 + 1 scenario. In the next section we present our study regarding the implications of one vanishing entry in the low energy neutrino mass matrix. We conclude in Sec. IV.

II. MASSES AND MIXING IN THE 3+1 SCHEME

There are two ways in which one can add a predominantly sterile state separated by $\sim eV^2$ from the standard three neutrino mass states. In the first case the additional neutrino can be of higher mass than the other three, while in the second case the fourth neutrino is the lightest state. The latter turns out to be incompatible with cosmology since in this case three active neutrinos, each with mass $\sim eV$, result in an enhanced cosmological energy density. Thus it suffices to consider only the first case which admits two possibilities, as displayed in Fig. 1.

- (i) SNH: In this case $m_1 \approx m_2 < m_3 < m_4$ corresponding to a normal hierarchy (NH) among the active neutrinos, which implies $m_2 = \sqrt{m_1^2 + \Delta m_{12}^2}$, $m_3 = \sqrt{m_1^2 + \Delta m_{12}^2 + \Delta m_{23}^2}$, $m_4 = \sqrt{m_1^2 + \Delta m_{14}^2}$.
- (ii) SIH: This corresponds to $m_3 < m_2 \approx m_1 < m_4$, implying an inverted ordering among the active neutrinos with masses expressed as $m_1 = \sqrt{m_3^2 + \Delta m_{13}^2}$, $m_2 = \sqrt{m_3^2 + \Delta m_{13}^2 + \Delta m_{12}^2}$, $m_4 = \sqrt{m_3^2 + \Delta m_{34}^2}$.
- Here, $\Delta m_{ij}^2 = m_j^2 - m_i^2$. We define the ratio of the mass squared differences ξ and ζ as

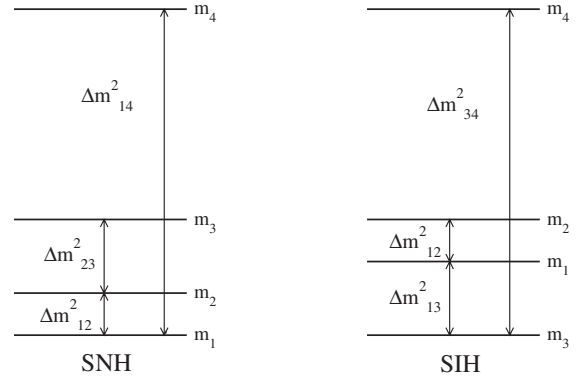


FIG. 1. The allowed 3 + 1 mass ordering.

$$\xi = \frac{\Delta m_{14}^2}{\Delta m_{23}^2} (\text{NH}) \quad \text{or} \quad \frac{\Delta m_{34}^2}{\Delta m_{13}^2} (\text{IH}), \quad (2)$$

$$\zeta = \frac{\Delta m_{12}^2}{\Delta m_{23}^2} (\text{NH}) \quad \text{or} \quad \frac{\Delta m_{12}^2}{\Delta m_{13}^2} (\text{IH}). \quad (3)$$

In extreme cases and using $\zeta \ll 1$, these masses can be written in terms of ξ and ζ as

$$\begin{aligned} \text{SNH: } |m_4| &\approx \sqrt{\Delta m_{23}^2 \xi} \gg |m_3| \approx \sqrt{(1 + \zeta) \Delta m_{23}^2} \\ &\approx \sqrt{\Delta m_{23}^2} \gg |m_2| \approx \sqrt{\Delta m_{23}^2 \zeta} \gg |m_1|, \end{aligned} \quad (4)$$

$$\begin{aligned} \text{SIH: } |m_4| &\approx \sqrt{\Delta m_{13}^2 \xi} \gg |m_2| \approx \sqrt{(1 + \zeta) \Delta m_{13}^2} \\ &\approx \sqrt{\Delta m_{13}^2} \approx |m_1| \gg |m_3|, \end{aligned} \quad (5)$$

$$\text{SQD: } |m_4| \gg |m_1| \approx |m_2| \approx |m_3| \approx m_0. \quad (6)$$

The first two cases correspond to a complete hierarchy among the active neutrinos, while the last one is the quasidegenerate (QD) regime where the three active neutrinos have approximately equal masses.

In the 3 + 1 scenario, the neutrino mixing matrix V in the flavor basis will be a 4×4 unitary matrix. In general, an $N \times N$ unitary mixing matrix contains $\frac{N(N-1)}{2}$ mixing angles and $\frac{1}{2}(N-1)(N-2)$ Dirac-type CP violating phases. It will also have $(N-1)$ additional Majorana phases if the neutrinos are Majorana particles. So in our case V can be parametrized in terms of 16 parameters. In addition to the three mixing angles between the active flavors, $(\theta_{13}, \theta_{12}, \theta_{23})$, we now have three more mixing angles from sterile and active mixing, $(\theta_{14}, \theta_{24}, \theta_{34})$. There are six CP violating phases, three Dirac $(\delta_{13}, \delta_{14}, \delta_{24})$ and three additional Majorana phases (α, β, γ) , as neutrinos here are considered to be Majorana particles. Then, there are four masses of the neutrino, m_1, m_2, m_3 corresponding to three active states and m_4 which is predominantly the mass of a heavy sterile neutrino.

TABLE I. The 3σ ranges of neutrino oscillation parameters [22]. The current constraints on sterile neutrino parameters are from [23,24], where $\Delta m_{\text{LSND}}^2 = \Delta m_{14}^2(\text{NH})$ or $\Delta m_{34}^2(\text{IH})$. Also given are the 3σ ranges of the mass ratios ζ and ξ .

Parameter	Best-fit values	3σ range
$\Delta m_{12}^2/10^{-5} \text{ eV}^2$ (NH or IH)	7.54	6.99–8.18
$\sin^2\theta_{12}/10^{-1}$ (NH or IH)	3.07	2.59–3.59
$\Delta m_{23}^2/10^{-3} \text{ eV}^2$ (NH)	2.43	2.19–2.62
$\Delta m_{13}^2/10^{-3} \text{ eV}^2$ (IH)	2.42	2.17–2.61
$\sin^2\theta_{13}/10^{-2}$ (NH)	2.41	1.69–3.13
$\sin^2\theta_{13}/10^{-2}$ (IH)	2.44	1.71–3.15
$\sin^2\theta_{23}/10^{-1}$ (NH)	3.86	3.31–6.37
$\sin^2\theta_{23}/10^{-1}$ (IH)	3.92	3.35–6.63
$\Delta m_{\text{LSND}}^2 \text{ eV}^2$	1.62	0.7–2.5
$\sin^2\theta_{14}$	0.03	0.01–0.06
$\sin^2\theta_{24}$	0.01	0.002–0.04
$\sin^2\theta_{34}$...	<0.18
$\zeta/10^{-2}$ (NH)	...	2.7–3.7
$\zeta/10^{-2}$ (IH)	...	2.7–3.8
$\xi/10^3$ (NH)	...	0.27–1.14
$\xi/10^3$ (IH)	...	0.27–1.15

The mixing matrix V can be expressed as $V = U.P$ [21], where

$$U = R_{34}\tilde{R}_{24}\tilde{R}_{14}R_{23}\tilde{R}_{13}R_{12}, \quad (7)$$

with R_{ij} denoting the rotation matrices in the ij generation space, expressed as

$$R_{34} = \begin{pmatrix} 1 & 0 & 0 & 0 \\ 0 & 1 & 0 & 0 \\ 0 & 0 & c_{34} & s_{34} \\ 0 & 0 & -s_{34} & c_{34} \end{pmatrix},$$

$$\tilde{R}_{14} = \begin{pmatrix} c_{14} & 0 & 0 & s_{14}e^{-i\delta_{14}} \\ 0 & 1 & 0 & 0 \\ 0 & 0 & 1 & 0 \\ -s_{14}e^{i\delta_{14}} & 0 & 0 & c_{14} \end{pmatrix}.$$

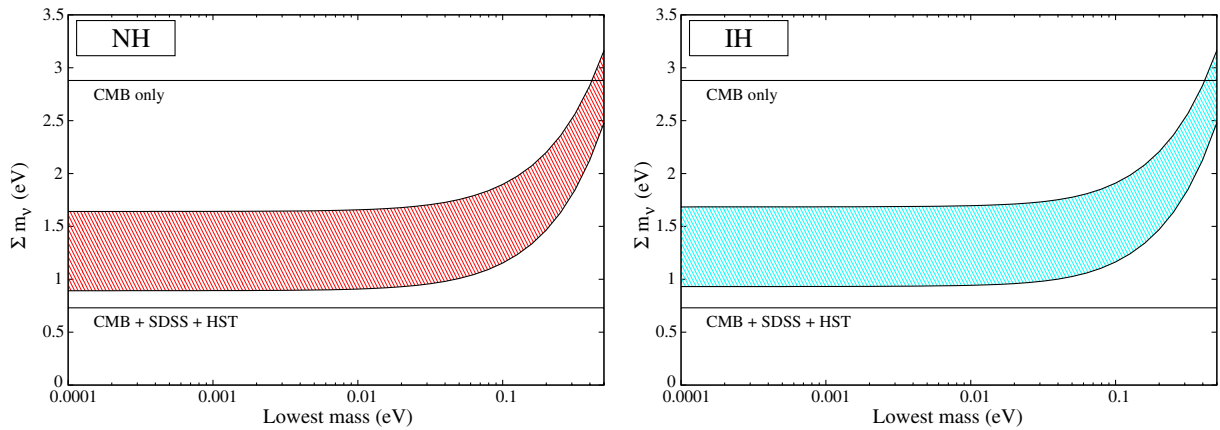


FIG. 2 (color online). Plots of the sum of light neutrino masses (Σm_ν) vs the lowest mass in the 3 + 1 scenario. Also shown are the cosmological upper bound on the neutrino mass from the analysis of CMB data plus matter power spectrum information (SDSS) and a prior on H_0 (HST), and from the analysis of CMB data only from Ref. [23] for the 3 + 1 scheme.

Here we use the abbreviations $s_{ij} = \sin \theta_{ij}$ and $c_{ij} = \cos \theta_{ij}$. The phase matrix is diagonal and is expressed as

$$P = \text{Diag}(1, e^{i\alpha}, e^{i(\beta+\delta_{13})}, e^{i(\gamma+\delta_{14})}).$$

The best-fit values and the 3σ ranges of the oscillation parameters in the 3 + 1 scenario are given in Table I, where in addition to the masses and mixing angles we also present the mass ratios ζ and ξ , which would be useful in our analysis. Note that the constraints on the three-neutrino parameters may change slightly once a full four-neutrino fit combining all global data is done. However, since the sterile mixing angles are small the change is not expected to be significant. Therefore, in the absence of a full four-neutrino global fit we use three-neutrino parameter values as obtained from three-generation analyses [22,25,26].

In Fig. 2 we have plotted the sum of the neutrino masses against the lowest neutrino mass for both NH and inverted hierarchy (IH). The band corresponds to variation of the mass squared differences in their current, e 3σ range. We also show the cosmological upper bound on neutrino masses in the 3 + 1 scenario from [23]. The combined analysis of CMB + SDSS + HST seems to rule out the mass spectrum of the 3 + 1 scenario in the framework of standard cosmology. However, if only CMB data are taken into account, then the region for the lowest mass $<0.4 \text{ eV}$ is allowed for both the hierarchies. Note that the analysis in [23] does not incorporate the Planck results [11], which can constrain the sum of masses further. In our analysis we have varied the lowest mass up to 0.5 eV .

III. NEUTRINO MASS MATRIX ELEMENTS

In this section we study the implication of the condition of vanishing $m_{\alpha\beta}$ for the 3 + 1 scenario, where $\alpha, \beta = e, \mu, \tau, s$. Since $m_{\alpha\beta}$ is complex the above condition implies that both real and imaginary parts are zero. Therefore, to study the one-zero textures we consider $|m_{\alpha\beta}| = 0$. In our

analysis we have varied the three Dirac phases in the range 0 to 2π and the three Majorana phases from 0 to π .

A. The mass matrix element m_{ee}

The matrix element m_{ee} in the 3 + 1 scenario is given as

$$m_{ee} = m_1 c_{14}^2 c_{13}^2 c_{12}^2 + m_2 s_{12}^2 c_{14}^2 c_{13}^2 e^{2i\alpha} + m_3 s_{13}^2 c_{14}^2 e^{2i\beta} + m_4 s_{14}^2 e^{2i\gamma}. \quad (8)$$

This can be written in the form

$$m_{ee} = c_{14}^2 (m_{ee})_{3\nu} + e^{2i\gamma} s_{14}^2 m_4, \quad (9)$$

where $(m_{ee})_{3\nu}$ corresponds to the matrix element in the case of three active neutrinos. The contribution of the sterile neutrino to the element m_{ee} depends on the mass m_4 and the active-sterile mixing angle θ_{14} . Of all the mass matrix elements, m_{ee} has the simplest form because of the chosen parametrization, and it can be understood quite well. Using the approximation in Eq. (4) for the case of extreme hierarchy, one can write this element for NH as

$$m_{ee} \approx c_{14}^2 (m_{ee})_{3\nu} + e^{2i\gamma} s_{14}^2 \sqrt{\Delta m_{14}^2}, \quad (10)$$

where $(m_{ee})_{3\nu} \approx \sqrt{\Delta m_{23}^2} (e^{2i\alpha} c_{13}^2 s_{12}^2 \sqrt{\xi} + s_{13}^2 e^{2i\beta})$ and ξ is defined in Eq. (3). The modulus of m_{ee} is the effective mass that can be extracted from half-life measurements in neutrinoless double beta decay. In Fig. 3 we plot the effective mass as a function of the smallest mass by varying θ_{14} in its complete 3σ range from Table I, as well as for specific values of the mixing angle θ_{14} . The Majorana phases are varied randomly in the range 0 to π in all the plots. The first panel is for $\theta_{14} = 0$, i.e., the three-generation case. We see that for present values of the oscillation parameters the cancellation condition is not satisfied for $m_1 \rightarrow 0$ for NH. However, as one increases m_1 , complete cancellation can be achieved. For IH the complete cancellation is never possible. These results change when we include the sterile contribution, as is evident from panel (b) in Fig. 3 which shows the effective mass for NH and IH by varying all the parameters in the full 3σ allowed range. The behavior can be understood from the expressions of $|m_{ee}|$ in various limiting cases. For NH, in the hierarchical limit of $m_1 \rightarrow 0$, the major contributor will be the additional term due to the sterile neutrinos because of a higher value of m_4 . Complete cancellation is only possible for smaller values of θ_{14} , so this contribution is suppressed. The typical value of θ_{14}

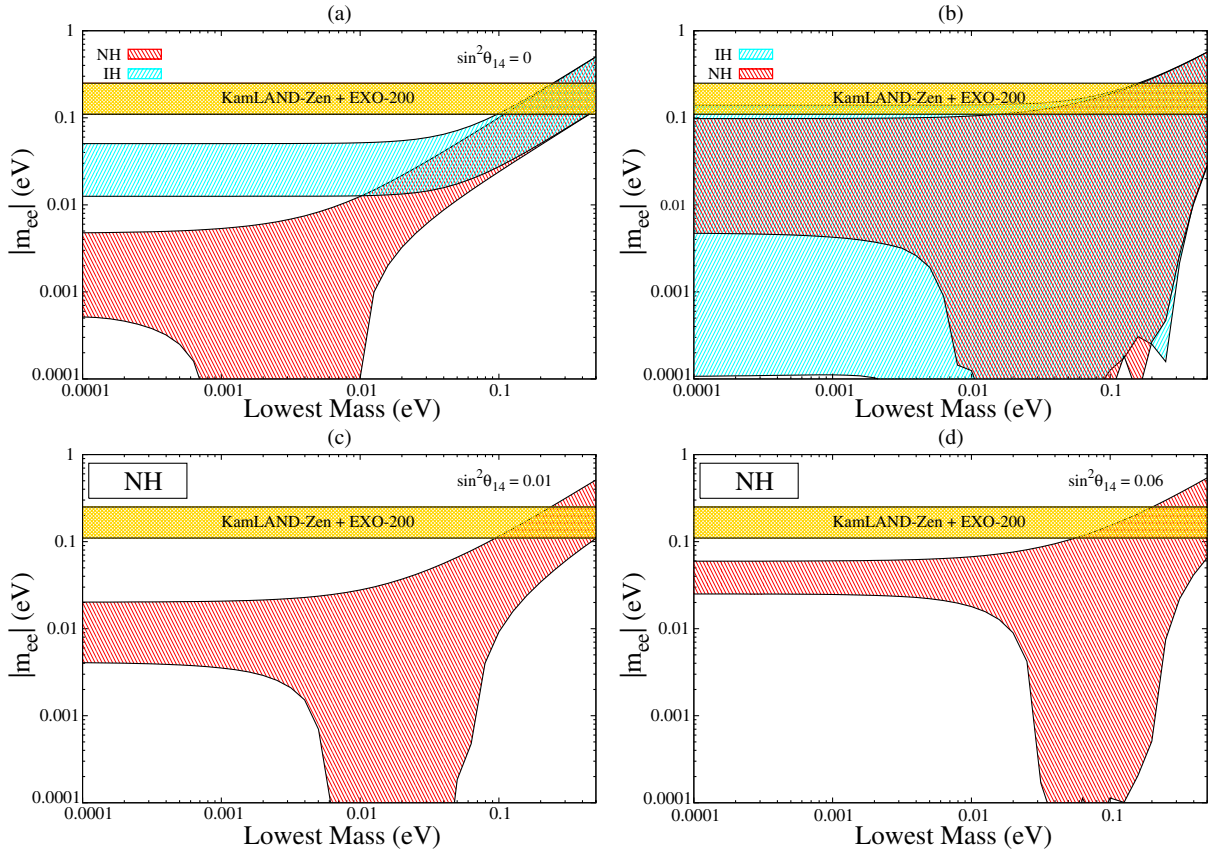


FIG. 3 (color online). Plot of $|m_{ee}|$ vs the lowest mass. Panel (a) corresponds to the three-generation case, while panel (b) is for the 3 + 1 case. In panel (b) all the mixing angles are varied in the 3σ range, and the Majorana CP violating phases are varied in their full range ($0-\pi$). Panels (c) and (d) are for specific values of θ_{14} , with all other parameters covering their full range.

required for cancellation can be obtained by putting $\alpha = \beta = 0$ (which would maximize the three-neutrino contribution) and $\gamma = \pi/2$, as

$$\tan^2 \theta_{14} \approx \frac{(\sqrt{\xi} c_{13}^2 s_{12}^2 + s_{13}^2)}{\sqrt{\xi}} \approx 10^{-3}, \quad (11)$$

which lies outside the allowed range of θ_{14} given in Table I. As we increase m_1 , $(m_{ee})_{3\nu}$ increases and can be of the same order of magnitude as the sterile term. Hence one can obtain cancellation regions. The cancellation is mainly controlled by the value of θ_{14} . For higher values of s_{14}^2 one needs a higher value of m_1 for cancellation to occur. This correlation between m_1 and θ_{14} is shown in panels (c) and (d) in Fig. 3.

For the IH case, in the limit of vanishing m_3 using the approximation in Eq. (5), m_{ee} in a 3 + 1 scenario can be written as

$$|m_{ee}| \approx |c_{14}^2 c_{13}^2 \sqrt{\Delta m_{13}^2} (c_{12}^2 + s_{12}^2 e^{2i\alpha}) + \sqrt{\Delta m_{34}^2} s_{14}^2 e^{2i\gamma}|. \quad (12)$$

The maximum value is achieved for $\alpha = \gamma = 0$, which is slightly lower than that of NH in this limit. The element vanishes in the limit $m_3 \approx 0$ eV when $\alpha = 0$ and $\gamma = \pi/2$, provided

$$\tan^2 \theta_{14} \approx \frac{c_{13}^2}{\sqrt{\xi}} \approx 0.05. \quad (13)$$

This is well within the allowed range. This behavior is in stark contrast to that in the three-neutrino case [27]. There is no significant change in this behavior as the

smallest mass m_3 is increased since this contribution is suppressed by the s_{13}^2 term and the dominant contribution to $(m_{ee})_{3\nu}$ comes from the first two terms in Eq. (8). Therefore, in this case we do not observe any correlation between m_3 and s_{14}^2 .

While moving towards the quasidegenerate regime of $m_1 \approx m_2 \approx m_3$, we find that the effective mass can still be zero. However, when the lightest mass approaches a larger value close to 0.3 eV, we need very large values of the active sterile mixing angle θ_{14} , outside the allowed range, for cancellation. Hence the effective mass cannot vanish for such mass values.

Also shown is the current limit on the effective mass from combined KamLAND-Zen and EXO 200 results on the half-life of $0\nu\beta\beta$ in ^{136}Xe [28,29]. When translated in terms of the effective mass, this corresponds to the bound $|m_{ee}| < 0.11\text{--}0.24$ eV, including nuclear matrix element uncertainties. For the three-generation case, the hierarchical neutrinos cannot saturate this bound. But in the 3 + 1 scenario this bound can be reached even for very small values of m_3 for IH, and for some parameter values it can even exceed the current limit. Thus, from the present limits on neutrinoless double beta decay searches, a part of the parameter space for smaller values of m_3 can be disfavored for IH. For NH the KamLAND-Zen + EXO 200 combined bound is reached for $m_1 = 0.02$ eV, and again some part of the parameter space can be disfavored by this bound.

B. The mass matrix element $m_{e\mu}$

The mass matrix element $m_{e\mu}$ in the presence of an extra sterile neutrino is given as

$$\begin{aligned} m_{e\mu} = & c_{14}(e^{i(\delta_{14}-\delta_{24}+2\gamma)} m_4 s_{14} s_{24} + e^{i(\delta_{13}+2\beta)} m_3 s_{13} (c_{13} c_{24} s_{23} - e^{i(\delta_{14}-\delta_{13}-\delta_{24})} s_{13} s_{14} s_{24})) \\ & + c_{12} c_{13} m_1 (-c_{23} c_{24} s_{12} + c_{12} (-e^{i\delta_{13}} c_{24} s_{13} s_{23} - e^{i(\delta_{14}-\delta_{24})} c_{13} s_{14} s_{24})) \\ & + e^{2i\alpha} m_2 c_{13} s_{12} (c_{12} c_{23} c_{24} + s_{12} (-e^{i\delta_{13}} c_{24} s_{13} s_{23} - e^{i(\delta_{14}-\delta_{24})} c_{13} s_{14} s_{24})). \end{aligned} \quad (14)$$

Unlike m_{ee} , here the expression is complicated, and an analytic understanding is difficult for the full expression. The expression for $m_{e\mu}$ in the limit of the vanishing active sterile mixing angle θ_{24} becomes

$$m_{e\mu} = c_{14}(m_{e\mu})_{3\nu}.$$

Since the active sterile mixing is small, in order to simplify these expressions we introduce a quantity $\lambda \equiv 0.2$ and define these small angles to be of the form $a\lambda$. Thus a systematic expansion in terms of λ can be done. For the sterile mixing angle

$$\sin \theta_{14} \approx \theta_{14} \equiv \chi_{14}\lambda, \quad \sin \theta_{24} \approx \theta_{24} \equiv \chi_{24}\lambda, \quad (15)$$

and for the reactor mixing angle

$$\sin \theta_{13} \approx \theta_{13} \equiv \chi_{13}\lambda. \quad (16)$$

Here χ_{ij} are parameters of $\mathcal{O}(1)$, and their 3σ range from the current constraint on the mixing angles is given by

$$\chi_{13} = 0.65\text{--}0.9, \quad \chi_{14} = 0.5\text{--}1.2, \quad \chi_{24} = 0.25\text{--}1. \quad (17)$$

Note that for the sterile mixing angle θ_{34} we do not adopt the above approximation because this angle can be large compared to the other two sterile mixing angles, and hence the small parameter approximation will not be valid.

Using the approximation in Eqs. (4), (15), and (16) we get the expression for $|m_{e\mu}|$ for normal hierarchy as

$$\begin{aligned} |m_{e\mu}| \approx & |\sqrt{\Delta m_{23}^2} \{ \sqrt{\xi} s_{12} c_{12} c_{23} e^{2i\alpha} \\ & + e^{i\delta_{13}} (e^{2i\beta} - e^{2i\alpha} \sqrt{\xi} s_{12}^2) s_{23} \lambda \chi_{13} \\ & + \lambda^2 e^{i(\delta_{14}-\delta_{24})} (e^{2i\gamma} \sqrt{\xi} - e^{2i\alpha} \sqrt{\xi} s_{12}^2) \chi_{14} \chi_{24} \}|. \end{aligned} \quad (18)$$

To see the order of magnitude of the different terms, we choose vanishing Majorana phases, while Dirac CP phases are taken as π . The mass matrix element $m_{e\mu}$ vanishes when

$$\begin{aligned} & \sqrt{\xi} s_{12} c_{12} c_{23} - (1 - \sqrt{\xi} s_{12}^2) s_{23} \lambda \chi_{13} \\ & + \lambda^2 (\sqrt{\xi} - \sqrt{\xi} s_{12}^2) \chi_{14} \chi_{24} = 0. \end{aligned} \quad (19)$$

The three-generation limit is recovered for $s_{24}^2 = 0$, and in panel (a) of Fig. 4 we show $|m_{e\mu}|$ as a function of m_1 for NH. Panel (b) (red/light region) of Fig. 4 shows $|m_{e\mu}|$ for the $3 + 1$ case, with all parameters varied randomly within their 3σ range. The figures show that $|m_{e\mu}| = 0$ can be achieved over the whole range of the smallest mass for both the 3 and $3 + 1$ cases. However, we find that in the hierarchical limit cancellation is not achieved for large values of θ_{24} , since in that case the third term of Eq. (19) will be of the order $\mathcal{O}(10^{-1})$ compared to the leading order term which is of the order $\mathcal{O}(10^{-2})$, and hence there will be no cancellation of these terms. This can be seen from panel (b) (green/dark region) of Fig. 4 for $s_{24}^2 = 0.04$. In the QD limit the contributions from the active terms are large enough to cancel the sterile contribution, and thus $|m_{e\mu}| = 0$ can be achieved.

For IH, using the approximation in Eq. (5) for the hierarchical limit, we get the expression

$$\begin{aligned} |m_{e\mu}| \approx & \left| \sqrt{\Delta m_{13}^2} \{ c_{12} s_{12} c_{23} (e^{2i\alpha} - 1) \right. \\ & - e^{i\delta_{13}} (c_{12}^2 + s_{12}^2 e^{2i\alpha}) s_{23} \chi_{13} \lambda \\ & \left. - e^{i(\delta_{14} - \delta_{24})} \lambda^2 \chi_{14} \chi_{24} (c_{12}^2 - e^{2i\gamma} \sqrt{\xi} + e^{2i\alpha} s_{12}^2) \right|. \end{aligned} \quad (20)$$

To see the order of magnitude of the various terms, we consider the case when Majorana phases vanish and the

Dirac phases assume the value π . Then we get, for vanishing $m_{e\mu}$,

$$s_{23} \lambda \chi_{13} - \lambda^2 (1 - \sqrt{\xi}) \chi_{14} \chi_{24} = 0. \quad (21)$$

In panel (a) of Fig. 5 we display the plot of $|m_{e\mu}|$ with m_3 for the three-generation scenario, i.e., for $\sin^2 \theta_{24} = 0$ for IH. In panel (b) we consider the $3 + 1$ case with all the parameters varying in their allowed range. Note that in the small m_3 limit [cf. Eq. 3.13] for $\alpha = 0$ the leading order term vanishes. For this case, for the large active sterile mixing angle θ_{24} , the λ^2 term becomes large [$\mathcal{O}(10^{-1})$], and cancellation with the λ term is not possible. When the CP violating phase α is nonzero, the leading order term can cancel the λ^2 term even for large values of s_{24}^2 . These features are reflected in panel (c), where we plot $|m_{e\mu}|$ for $s_{24}^2 = 0.04$ and $\alpha = 0$ (blue/dark region) and by varying α in its full range (cyan/light region). As expected, for $\alpha = 0$, cancellation is not achieved for smaller values of m_3 . Thus the condition $|m_{e\mu}| = 0$ implies some correlation between m_3 and α for IH. Even if α is varied in its full range, the absolute value of the matrix element $|m_{e\mu}|$ can vanish only if the product $\chi_{14} \chi_{24}$ is small, i.e., s_{14}^2 and s_{24}^2 are simultaneously small. This is because if they are large the λ^2 term becomes of the order $\mathcal{O}(10^{-1})$, and hence cancellation will not be possible. This is seen in panel (d), where for $s_{14}^2 = 0.06$ and $s_{24}^2 = 0.04$ the region where m_3 is small becomes disallowed. Taking CP violating phase $\alpha = \pi/2$ makes the magnitude of the leading order term ($s_{12} c_{12} c_{23} \sqrt{\xi}$) quite large, and smaller values of θ_{24} cannot cause a cancellation even for large values of m_3 , which can be seen from panel (e) of Fig. 5. For the occurrence of cancellation s_{24}^2 has to be ≥ 0.01 for $\alpha = \pi/2$, as can be seen from panel (f), where we have plotted the correlation between α and s_{24}^2 for $|m_{e\mu}| = 0$.

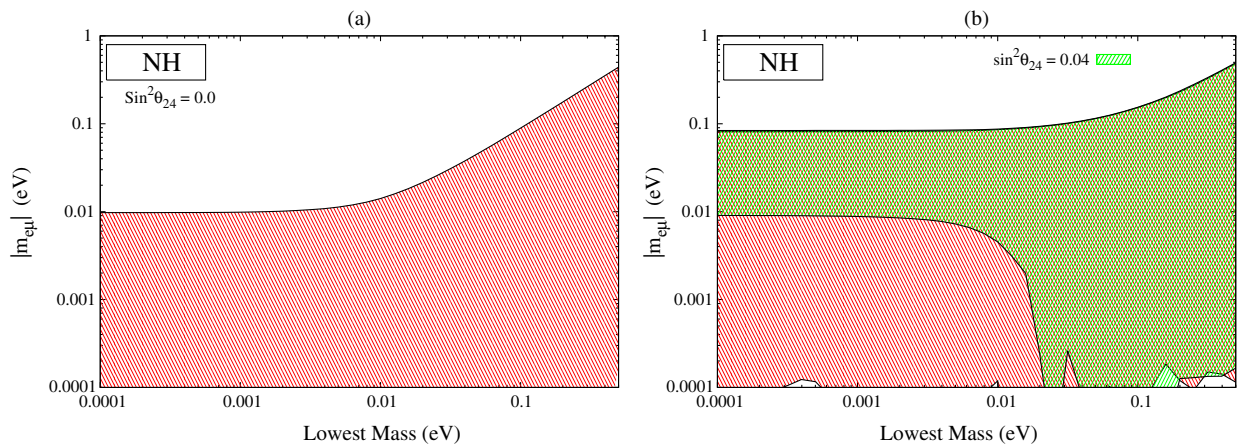


FIG. 4 (color online). Plots of $|m_{e\mu}|$ as a function of the lowest mass m_1 for NH. Panel (a) corresponds to the three-generation case, while (b) (red/light region) is for the $3 + 1$ case and also for $s_{24}^2 = 0.04$ (green/dark region). All the parameters are varied in their full 3σ allowed range; the CP violating Dirac phases are varied from 0 to 2π , and the Majorana phases are varied from 0 to π unless otherwise stated.

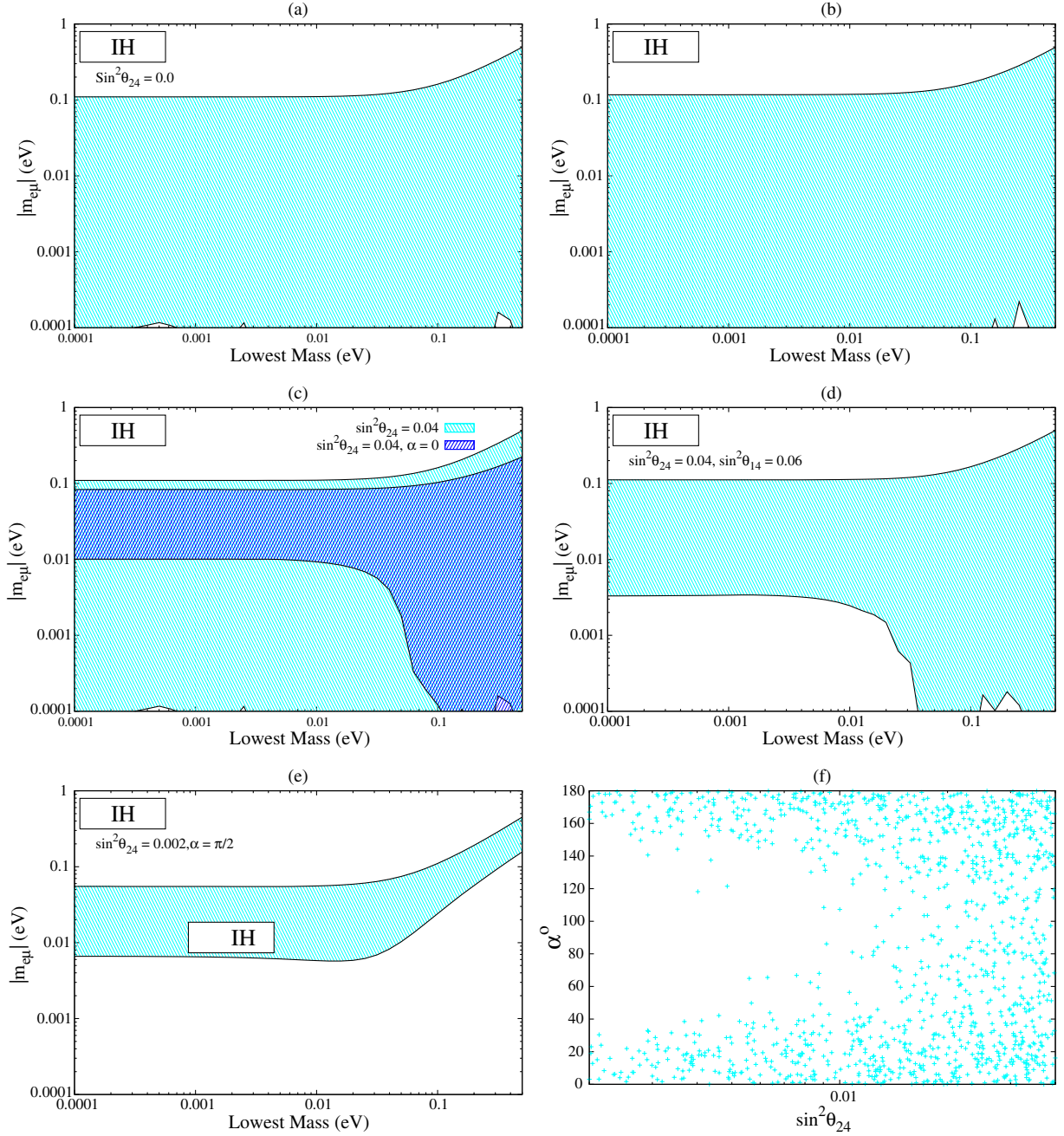


FIG. 5 (color online). Plots of $|m_{e\mu}|$ vs m_3 for inverted hierarchy for (a) the three-generation case and (b) the 3 + 1 case with all parameters varied randomly in their full range. Panels (c), (d), and (e) are for specific values of s_{24}^2 and α . Panel (f) shows the correlation between α and s_{24}^2 when all other parameters are randomly varied.

C. The mass matrix element $m_{e\tau}$

The mass matrix element $m_{e\tau}$, in the presence of an extra sterile neutrino, is given by

$$\begin{aligned}
 m_{e\tau} = & c_{14}c_{24}e^{i(2\gamma+\delta_{14})}m_4s_{14}s_{34} + m_3c_{14}s_{13}e^{i(2\beta+\delta_{13})}(-c_{24}s_{13}s_{14}s_{34}e^{i(\delta_{14}-\delta_{13})} + c_{13}(c_{23}c_{34} - e^{i\delta_{24}}s_{23}s_{24}s_{34})) \\
 & + m_2s_{12}c_{13}c_{14}e^{2i\alpha}(c_{12}(-c_{34}s_{23} - c_{23}s_{24}s_{34}e^{i\delta_{24}}) + s_{12}(-c_{13}c_{24}s_{14}s_{34}e^{i\delta_{14}} - e^{i\delta_{13}}s_{13}(c_{23}c_{34} - e^{i\delta_{24}}s_{23}s_{24}s_{34}))) \\
 & + m_1c_{12}c_{13}c_{14}(-s_{12}(-c_{34}s_{23} - c_{23}s_{24}s_{34}e^{i\delta_{24}}) + c_{12}(-c_{13}c_{24}s_{14}s_{34}e^{i\delta_{14}} - e^{i\delta_{13}}s_{13}(c_{23}c_{34} - e^{i\delta_{24}}s_{23}s_{24}s_{34}))). \quad (22)
 \end{aligned}$$

The elements $m_{e\tau}$ and $m_{e\mu}$ are related by $\mu - \tau$ permutation symmetry,

$$P_{\mu\tau} = \begin{pmatrix} 1 & 0 & 0 & 0 \\ 0 & 0 & 1 & 0 \\ 0 & 1 & 0 & 0 \\ 0 & 0 & 0 & 1 \end{pmatrix},$$

in such a way that

$$m_{e\tau} = P_{\mu\tau}^T m_{e\mu} P_{\mu\tau}.$$

For the case of three active neutrinos the mixing angle θ_{23} in the partner textures linked by $\mu - \tau$ symmetry is related as $\bar{\theta}_{23} = (\frac{\pi}{2} - \theta_{23})$. However, in the $3 + 1$ case the relation of θ_{23} between two textures related by this symmetry is not simple. The active sterile mixing angles θ_{24} and θ_{34} are also different in the textures connected by $\mu - \tau$ symmetry and are related as [17]

$$\bar{\theta}_{12} = \theta_{12}, \quad \bar{\theta}_{13} = \theta_{13}, \quad \bar{\theta}_{14} = \theta_{14}, \quad (23)$$

$$\sin \bar{\theta}_{24} = \sin \theta_{34} \cos \theta_{24}, \quad (24)$$

$$\sin \bar{\theta}_{23} = \frac{\cos \theta_{23} \cos \theta_{34} - \sin \theta_{23} \sin \theta_{34} \sin \theta_{24}}{\sqrt{1 - \cos \theta_{24}^2 \sin \theta_{34}^2}}, \quad (25)$$

$$\sin \bar{\theta}_{34} = \frac{\sin \theta_{24}}{\sqrt{1 - \cos \theta_{24}^2 \sin \theta_{34}^2}}. \quad (26)$$

Because of these relations the behavior of $m_{e\mu}$ is different from that of $m_{e\tau}$, unlike in the three-active-neutrino case where the plots of these two elements are the same except for θ_{23} which differed in octant for the two cases.

It is found that in the limit of small θ_{24} , the two active sterile mixing angles $\bar{\theta}_{24}$ and θ_{34} are approximately equal, as can be seen from Eq. (24). The same can be seen from Eq. (26), which gives $\bar{\theta}_{34} \approx \theta_{24}$ for smaller values of the mixing angle θ_{34} . Thus, for these cases the behavior shown by θ_{24} in $m_{e\mu}$ ($m_{\mu\mu}$) is the same as that shown by θ_{34} in $m_{e\tau}$ ($m_{\tau\tau}$).

In the limit of the vanishing active sterile mixing angle θ_{34} , this element becomes

$$m_{e\tau} = c_{14}(m_{e\tau})_{3\nu}.$$

Using the approximation in Eq. (4) for NH, the above element can be expressed as

$$|m_{e\tau}| \approx |\sqrt{\Delta m_{23}^2} \{-s_{12}s_{23}c_{12}c_{34}\sqrt{\xi}e^{2i\alpha} + \lambda(c_{23}c_{34}e^{i(2\beta+\delta_{13})}\chi_{13} - c_{23}c_{34}s_{12}^2\chi_{13}\sqrt{\xi}e^{i(2\alpha+\delta_{13})} + e^{i(2\gamma+\delta_{14})}\sqrt{\xi}s_{34}\chi_{14} - e^{i(2\alpha+\delta_{14})}\sqrt{\xi}s_{12}^2s_{34}\chi_{14} - c_{12}c_{23}e^{i(2\alpha+\delta_{24})}s_{12}s_{34}\chi_{24}\sqrt{\xi}\} - e^{i(\delta_{13}+\delta_{24})}(e^{2i\beta} - e^{2i\alpha}s_{12}^2\sqrt{\xi})s_{23}s_{34}\chi_{13}\chi_{24}\lambda^2}|. \quad (27)$$

For the case of vanishing Majorana phases and Dirac phases having the value π , this element can vanish when

$$-c_{12}c_{34}\sqrt{\xi}s_{12}s_{23} - (1 - \sqrt{\xi}s_{12}^2)s_{23}s_{34}\lambda^2\chi_{13}\chi_{24} + \lambda(-c_{23}c_{34}\chi_{13} + \sqrt{\xi}c_{23}s_{12}(c_{34}s_{12}\chi_{13} + c_{12}s_{34}\chi_{24}) + s_{12}^2s_{34}\chi_{14}\sqrt{\xi} - \sqrt{\xi}s_{34}\chi_{14}) = 0. \quad (28)$$

For a vanishing active sterile mixing angle θ_{34} one recovers the three-generation case. In this limit, from Eq. (28) one observes that the leading order term and the term with λ are of the same order, $\sim \mathcal{O}(10^{-2})$, while the λ^2 term vanishes and hence cancellation is possible except for very low values of the lightest mass. We can see this in panel (a) of Fig. 6. In panel (b) (red/light region) all the parameters are varied randomly ($3 + 1$ case), and cancellation is seen to be possible over the whole range of m_1 . In panel (b) (green/dark region) we also plot the element $|m_{e\tau}|$ for the upper limit of $s_{34}^2 = 0.18$. In this case there is no cancellation for very low values of the smallest mass. This is because when s_{34}^2 is large, the λ term containing ξ becomes large $\mathcal{O}(1)$ and there will be no cancellation. For inverted hierarchy the element $m_{e\tau}$, using the approximation in Eq. (5), becomes

$$|m_{e\tau}| \approx |\sqrt{\Delta m_{13}^2} \{c_{12}c_{34}s_{12}s_{23}(-e^{2i\alpha} + 1) + e^{i(\delta_{13}+\delta_{24})}(c_{12}^2 + e^{2i\alpha}s_{12}^2)s_{23}s_{34}\lambda^2\chi_{13}\chi_{24} - \lambda(c_{23}c_{34}\chi_{13}e^{i\delta_{13}}(c_{12}^2 + e^{2i\alpha}s_{12}^2) + e^{i\delta_{14}}s_{34}\chi_{14}(c_{12}^2 + e^{i\alpha}s_{12}^2) - e^{i(2\gamma+\delta_{14})}s_{34}\chi_{14}\sqrt{\xi} + c_{12}c_{23}s_{12}s_{34}\chi_{24}e^{i\delta_{24}}(e^{2i\alpha} - 1))\}|. \quad (29)$$

In the limit of vanishing Majorana phases and Dirac CP violating phases equal to π , this element becomes negligible when

$$\lambda(c_{23}c_{34}\chi_{13} + s_{34}\chi_{14} - s_{34}\chi_{14}\sqrt{\xi}) + s_{23}s_{34}\chi_{13}\chi_{24}\lambda^2 = 0. \quad (30)$$

In panel (a) of Fig. 7 the three-generation case is reproduced by putting $s_{34}^2 = 0$, and in (b) all the parameters are varied in their allowed range ($3 + 1$ case). In both the figures we can see that cancellation is permissible over the whole range of m_3 considered. When the CP violating phase $\alpha = 0$, we see that the leading order term ($\sin 2\theta_{12}s_{23}c_{34}$) vanishes, and as a result for large values

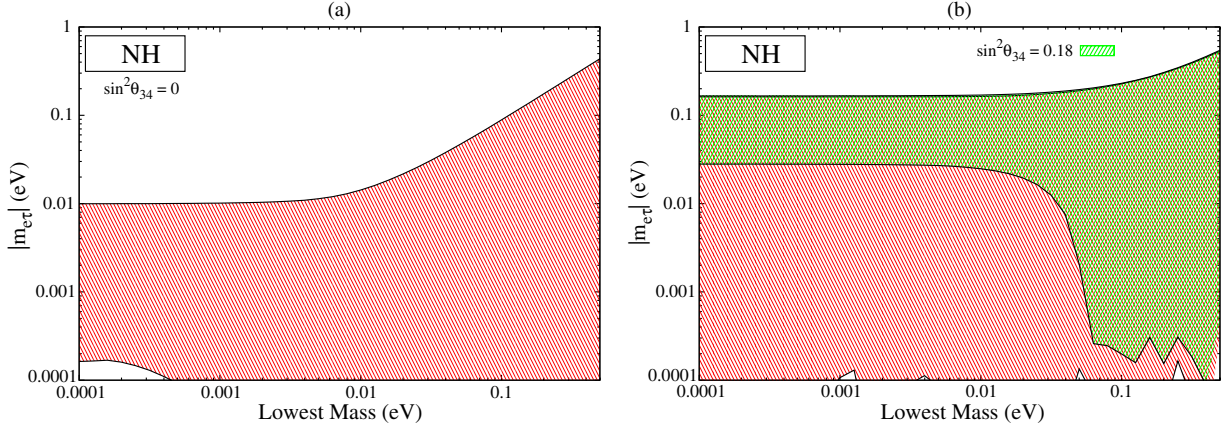


FIG. 6 (color online). Plots of $|m_{e\tau}|$ for normal hierarchy with the lowest mass m_1 . Panel (a) corresponds to the three-generation case. In (b) (red/light region) all the parameters are varied in their full allowed range, and the green/dark region is for $s_{34}^2 = 0.18$, with all the other parameters covering their full range.

of s_{34}^2 the cancellation is not possible because the term with the coefficient λ becomes large [$\mathcal{O}(10^{-1})$]. For nonzero values of the CP violating phase α , this leading order term is nonzero and its contribution will be significant. So in this case high values of θ_{34} are also allowed because now the leading order and the term with coefficient λ will be of the same magnitude. When we fix $s_{34}^2 = 0.06$ and $\alpha = 0$, the region where m_3 is small is disallowed [panel (c) blue/dark region], but when α varies within its full range the disallowed regions become allowed [panel (c) cyan/light region]. When s_{34}^2 approaches its upper limit, the λ term having ξ becomes very large and cancellation is not

possible even for nonzero values of α , which can be seen from panel (d). However, when $\alpha = \pi/2$, very small values of s_{34}^2 cannot give a cancellation, as the leading order term becomes large [panel (e)]. s_{34}^2 has to be ≥ 0.01 for the term to vanish, which can be seen from panel (f) where we plotted the correlation between α and s_{34}^2 for $|m_{e\tau}| = 0$.

D. The mass matrix element $m_{\mu\mu}$

The (2, 2) diagonal entry in the neutrino mass matrix is given as

$$\begin{aligned}
 m_{\mu\mu} = & e^{2i(\delta_{14}-\delta_{24}+\gamma)} c_{14}^2 m_4 s_{24}^2 + e^{2i(\delta_{13}+\beta)} m_3 (c_{13} c_{24} s_{23} - e^{i(\delta_{14}-\delta_{13}-\delta_{24})} s_{13} s_{14} s_{24})^2 \\
 & + m_1 \{-c_{23} c_{24} s_{12} + c_{12} (-e^{i\delta_{13}} c_{24} s_{13} s_{23} - e^{i(\delta_{14}-\delta_{24})} c_{13} s_{14} s_{24})\}^2 \\
 & + e^{2i\alpha} m_2 \{c_{12} c_{23} c_{24} + s_{12} (-e^{i\delta_{13}} c_{24} s_{13} s_{23} - e^{i(\delta_{14}-\delta_{24})} c_{13} s_{14} s_{24})\}^2.
 \end{aligned} \tag{31}$$

This expression reduces to its three-generation case if the mixing angle θ_{24} vanishes. Also, we can see from this expression that there is no dependence on the mixing angle θ_{34} . Using the approximation in Eqs. (4) this element can be simplified to the form

$$\begin{aligned}
 |m_{\mu\mu}| \approx & \left| \sqrt{\Delta m_{23}^2} \{c_{12}^2 c_{23}^2 e^{2i\alpha} \sqrt{\xi} + e^{i(\delta_{13}+2\beta)} s_{23}^2 - 2\lambda c_{12} c_{23} e^{i(\delta_{13}+2\alpha)} \sqrt{\xi} s_{12} s_{23} \chi_{13} + \lambda^2 \{e^{2i(\delta_{13}+\alpha)} \sqrt{\xi} s_{12}^2 s_{23}^2 \chi_{13}^2 \right. \\
 & \left. + e^{i(\delta_{14}-\delta_{24})} (e^{i(2\gamma+\delta_{14}-\delta_{24})} \sqrt{\xi} \chi_{24} - 2e^{2i\alpha} \sqrt{\xi} c_{12} c_{23} s_{12} \chi_{14}) \chi_{24}\} \right|.
 \end{aligned} \tag{32}$$

For the case of Majorana CP phases having the value 0 and the Dirac phases having the value π , this element vanishes when

$$\begin{aligned}
 & s_{23}^2 + c_{12}^2 c_{23}^2 \sqrt{\xi} + c_{12} s_{12} \sin 2\theta_{23} \sqrt{\xi} \lambda \chi_{13} \\
 & + \lambda^2 (s_{12}^2 s_{23}^2 \sqrt{\xi} \chi_{13}^2 - c_{23} \sin 2\theta_{12} \sqrt{\xi} \chi_{14} \chi_{24}) \\
 & + \sqrt{\xi} \chi_{24}^2 = 0.
 \end{aligned} \tag{33}$$

We know that for the case of three generations, the elements in the $\mu - \tau$ block are quite large and cannot vanish

for normal hierarchy. In panel (a) of Fig. 8 we can see that $|m_{\mu\mu}|$ cannot vanish in the small m_1 region for $s_{24}^2 = 0$, which is indeed the three-generation case. This is because the magnitude of the first two terms in Eq. (34) is quite large in this case, $\sim \mathcal{O}(10^{-1})$, and for cancellation to occur the term with coefficient λ^2 has to be of the same order. This is not possible when s_{24}^2 is small. However, when s_{24}^2 is varied in its full allowed range the contribution of the sterile part is enhanced, and this can cancel the active part, as can be seen from panel (b). Now to understand the dependence of $m_{\mu\mu}$ with θ_{24} , we note that if we

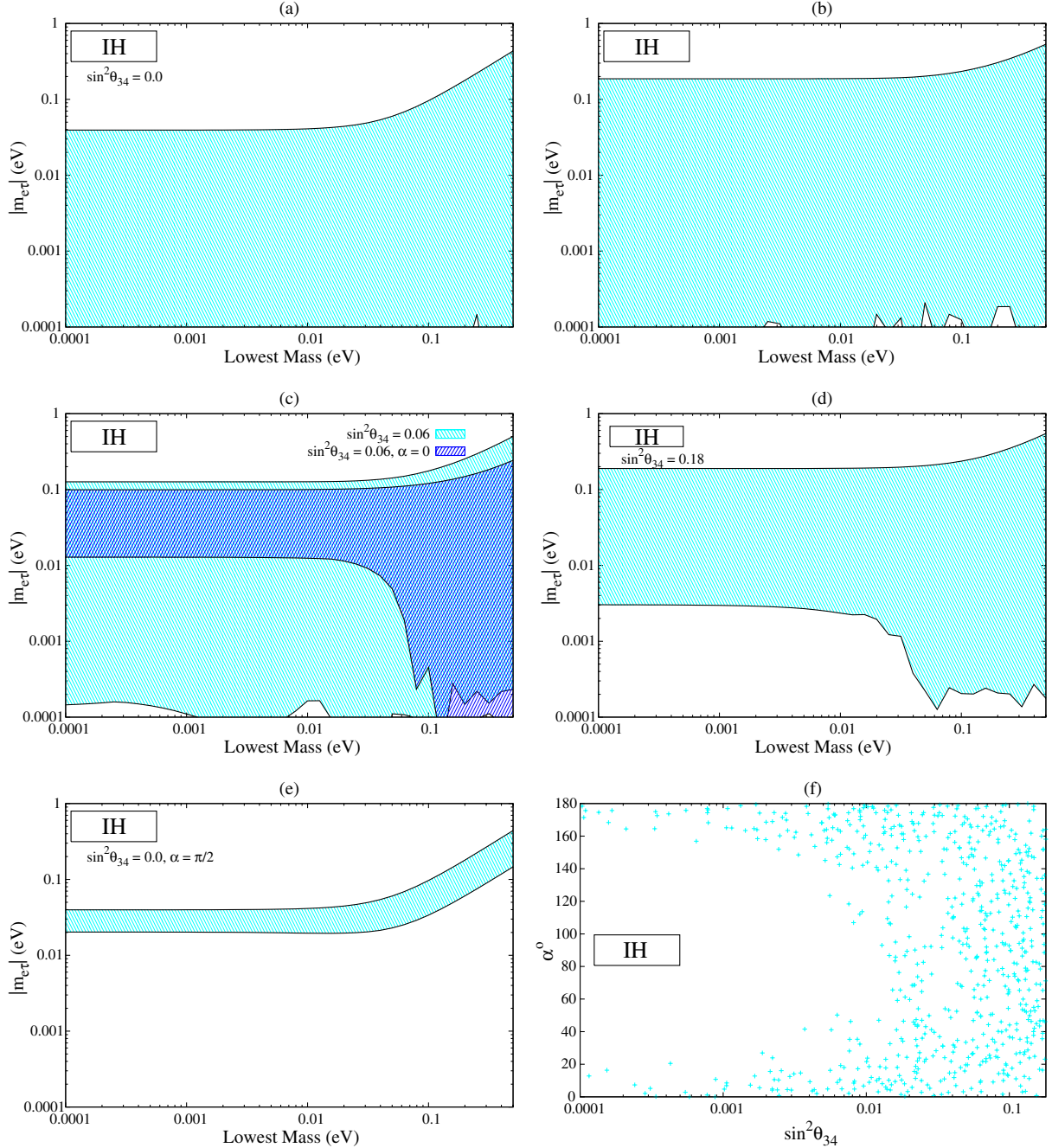


FIG. 7 (color online). Plots of $|m_{e\tau}|$ for inverted hierarchy with lowest mass m_3 . The panel (a) corresponds to three generation case. In (b) all the parameters are varied in their full allowed range (3 + 1). The panel (c), (d) is for specific value of θ_{34} and α with all the other parameters covering their full range. The panel (f) shows correlation between α and s_{34}^2 .

increase s_{24}^2 from its lower bound then the two terms become of the same order. So there will be regions in the limit of small m_1 for which this element vanishes [panel (c)]. We see in panel (d) of Fig. 8 that when θ_{24} acquires very large values, the magnitude of the λ^2 ($\sqrt{\xi}\chi_{24}^2$) term becomes large, thus leading to noncancellation of the terms with the first two leading order terms. Hence, the region with very small m_1 is not allowed. Using the approximation for inverted hierarchy the element $m_{\mu\mu}$ becomes

$$\begin{aligned}
 |m_{\mu\mu}| \approx & \left| \sqrt{\Delta m_{13}^2} \left[c_{23}^2 (s_{12}^2 + c_{12}^2 e^{2i\alpha}) \right. \right. \\
 & + \frac{1}{2} \lambda \sin 2\theta_{12} \sin 2\theta_{23} e^{i\delta_{13}} (1 - e^{2i\alpha}) \chi_{13} \\
 & + \lambda^2 [\sin 2\theta_{12} c_{23} e^{i(\delta_{14} - \delta_{24})} (1 - e^{2i\alpha}) \chi_{14} \chi_{24} \\
 & + s_{23}^2 e^{2i\delta_{13}} (c_{12}^2 + e^{2i\alpha} s_{12}^2) \chi_{13}^2 \\
 & \left. \left. + e^{2i(\gamma + \delta_{14} - \delta_{24})} \sqrt{\xi} \chi_{24}^2 \right] \right|. \quad (34)
 \end{aligned}$$

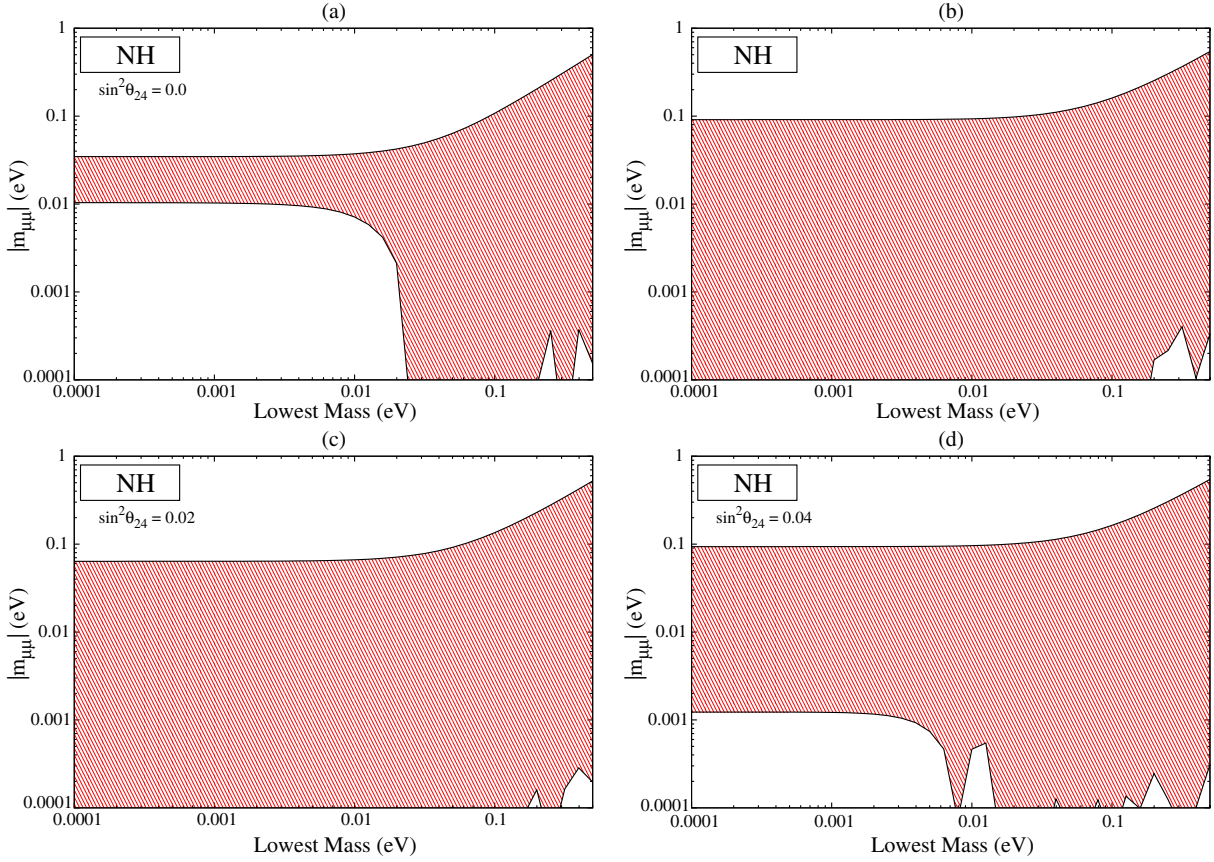


FIG. 8 (color online). Plots of vanishing $m_{\mu\mu}$ for normal hierarchy for different values of θ_{24} when all other mixing angles are varied in their 3σ ranges, Dirac CP phases are varied from 0 to 2π and Majorana phases from 0 to π .

Assuming Majorana phases are zero and Dirac phases have a value π , this element can vanish when

$$c_{23}^2 + \lambda^2(s_{23}^2\chi_{13}^2 + \sqrt{\xi}\chi_{24}^2) = 0. \quad (35)$$

In panel (a) of Fig. 9 we plotted $|m_{\mu\mu}|$ for $s_{24}^2 = 0$ to reproduce the three-generation case, whereas in panel (b) all the parameters are varied in their allowed range in the 3 + 1 scenario. In both cases we can see that cancellation is possible for the full range of m_3 . We notice that, unlike normal hierarchy, here cancellation is possible for small values of s_{24}^2 because in this case all the terms are of the same order and there can always be cancellations. However, if we put $\alpha = 0$ then the term $\lambda(\sin 2\theta_{12}s_{23}c_{23}\chi_{13})$ drops out from the equation and the leading order term cannot be canceled for small values of

s_{24}^2 . It can be seen from panel (c) that for $s_{24}^2 = 0.002$ and $\alpha = 0$ the regions where m_3 is small are not allowed. As the value of θ_{24} increases there is the possibility of cancellation of terms for all the values of α , as can be seen from panel (d) where we plot $|m_{\mu\mu}|$ with the lowest mass for $s_{24}^2 = 0.02$ when all the other mixing angles are varied in the 3σ range and CP violating phases are varied in the full range. Now if we keep increasing s_{24}^2 , then the λ^2 term will become large and the chance of cancellation will be less.

E. The mass matrix element $m_{\mu\tau}$

The (2, 3) element of M_ν in the flavor basis becomes quite complicated in the presence of an extra sterile neutrino. The expression is

$$\begin{aligned} m_{\mu\tau} = & e^{i(2\delta_{14}-\delta_{24}+2\gamma)}c_{14}^2c_{24}m_4s_{24}s_{34} + e^{2i(\delta_{13}+\beta)}m_3(c_{13}c_{24}s_{23} - e^{i(\delta_{14}-\delta_{24}-\delta_{13})}s_{13}s_{14}s_{24})\{-e^{i(\delta_{14}-\delta_{13})}c_{24}s_{13}s_{14}s_{34} \\ & + c_{13}(c_{23}c_{34} - e^{i\delta_{24}}s_{23}s_{24}s_{34})\} + m_1\{-c_{23}c_{24}s_{12} + c_{12}(-e^{i\delta_{13}}c_{24}s_{13}s_{23} - e^{i(\delta_{14}-\delta_{24})}c_{13}s_{14}s_{24})\} \\ & \times [-s_{12}(-c_{34}s_{23} - e^{i\delta_{24}}c_{23}s_{24}s_{34}) + c_{12}\{-e^{i\delta_{14}}c_{13}c_{24}s_{14}s_{34} - e^{i\delta_{13}}s_{13}(c_{23}c_{34} - e^{i\delta_{24}}s_{23}s_{24}s_{34})\}] \\ & + e^{2i\alpha}m_2\{c_{12}c_{23}c_{24} + s_{12}(-e^{i\delta_{13}}c_{24}s_{13}s_{23} - e^{i(\delta_{14}-\delta_{24})}c_{13}s_{14}s_{24})\}[c_{12}(-c_{34}s_{23} - e^{i\delta_{24}}c_{23}s_{24}s_{34}) \\ & + s_{12}\{-e^{i\delta_{14}}c_{13}c_{24}s_{14}s_{34} - e^{i\delta_{13}}s_{13}(c_{23}c_{34} - e^{i\delta_{24}}s_{23}s_{24}s_{34})\}]. \end{aligned} \quad (36)$$

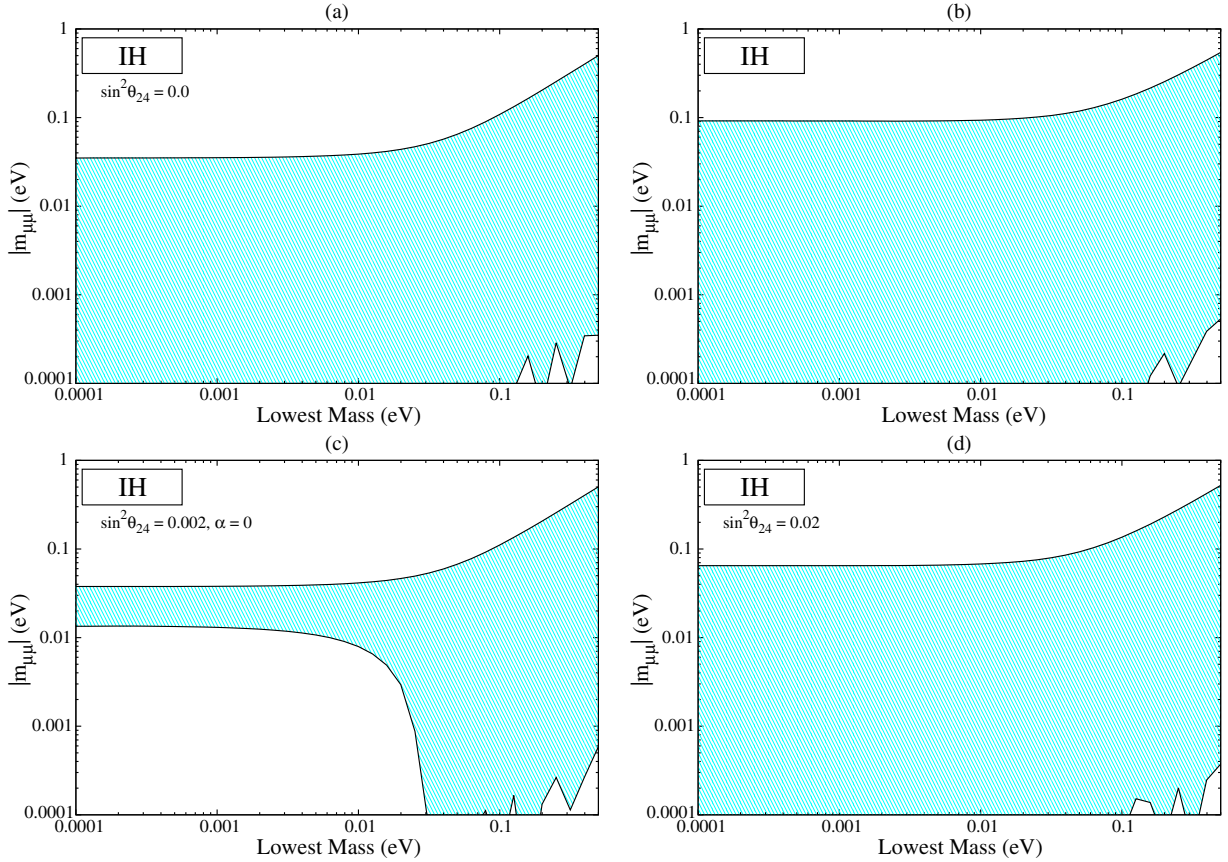


FIG. 9 (color online). Plots of vanishing $m_{\mu\mu}$ for inverted hierarchy with lowest mass m_3 . Panel (a) is for the three-generation case, and (b) shows that all the parameters are varied in the full allowed range (3 + 1). Panels (c) and (d) are for specific values of α and s_{24}^2 are taken with all other parameters covering their full range.

This reduces to the three-generation case when $\theta_{24} = \theta_{34} = 0$. In the normal hierarchical region where m_1 can assume very small values and can be neglected, using approximations in Eqs. (4), (15), and (16) we get

$$\begin{aligned}
 |m_{\mu\tau}| \approx & \sqrt{\Delta m_{23}^2} \{ c_{23}c_{34}(e^{2i(\beta+\delta_{13})} - e^{2i\alpha}\sqrt{\zeta}c_{12}^2)s_{23} - \lambda[c_{12}c_{34}e^{i(2\alpha+\delta_{13})}\sqrt{\zeta}s_{12}\cos 2\theta_{23}\chi_{13} \\
 & + e^{i\delta_{24}}(e^{2i\alpha}c_{12}^2c_{23}^2\sqrt{\zeta} + e^{2i(\beta+\delta_{13})}s_{23}^2)\chi_{24}s_{34} - e^{2i\delta_{14}}(e^{i(2\gamma-\delta_{24})}\sqrt{\xi}\chi_{24} - c_{12}c_{23}e^{2i\alpha}\sqrt{\zeta}s_{12}\chi_{14})s_{34} \\
 & + \lambda^2[\sqrt{\zeta}e^{i(2\alpha+\delta_{13})}(e^{i\delta_{14}}s_{12}\chi_{14} + 2c_{12}c_{23}e^{i\delta_{24}}\chi_{24})s_{12}s_{23}s_{34}\chi_{13} + e^{i\delta_{14}}(e^{i(2\alpha-\delta_{24})}c_{12}c_{34}\sqrt{\zeta}s_{12}\chi_{24} \\
 & - e^{i(2\beta+\delta_{13})}\chi_{13}s_{34})\chi_{14}s_{23} + c_{23}c_{34}e^{2i(\alpha+\delta_{13})}s_{12}^2\chi_{13}^2\sqrt{\zeta}s_{23}] \}. \quad (37)
 \end{aligned}$$

To see the order of the terms we consider the case where Majorana CP phases vanish and Dirac phases have the value π . In this limit the element becomes negligible when

$$\begin{aligned}
 c_{23}c_{34}s_{23}(1 - c_{12}^2\sqrt{\zeta}) + \lambda\{(c_{12}c_{34}s_{12}\sqrt{\zeta}\chi_{13})\cos 2\theta_{23} + \chi_{24}s_{34}(s_{23}^2 + c_{12}^2c_{23}^2\sqrt{\zeta}) + s_{34}(\sqrt{\xi}\chi_{24} + c_{12}c_{23}s_{12}\sqrt{\zeta}\chi_{14})\} \\
 + \lambda^2\{s_{12}\chi_{13}s_{23}s_{34}\sqrt{\zeta}(s_{12}\chi_{14} + 2c_{12}c_{23}\chi_{24}) + \chi_{14}s_{23}(c_{12}c_{34}s_{12}^2s_{23}\sqrt{\zeta}\chi_{13}^2)\} = 0. \quad (38)
 \end{aligned}$$

Being an element of the $\mu\tau$ block, $m_{\mu\tau}$ shows the same behavior as that of $m_{\mu\mu}$ in normal hierarchy. In panel (a) of Fig. 10 we plotted $|m_{\mu\tau}|$ for $s_{24}^2 = s_{34}^2 = 0$, which coincides with the three-generation case, and we can see that cancellation is not possible in the hierarchical region. However, when all the parameters are varied in their allowed range in panel (b), there is a contribution from the sterile part and

cancellation is always possible. It can also be seen from panel (c) of Fig. 10 that for $s_{34}^2 = 0$ there is no cancellation in the region when m_1 is small, and the figure is quite similar to that of the three-generation case. However, as this active sterile mixing angle becomes larger there is always the possibility of an allowed region towards the lower values of m_1 as is evident from panel (d). This is because for the

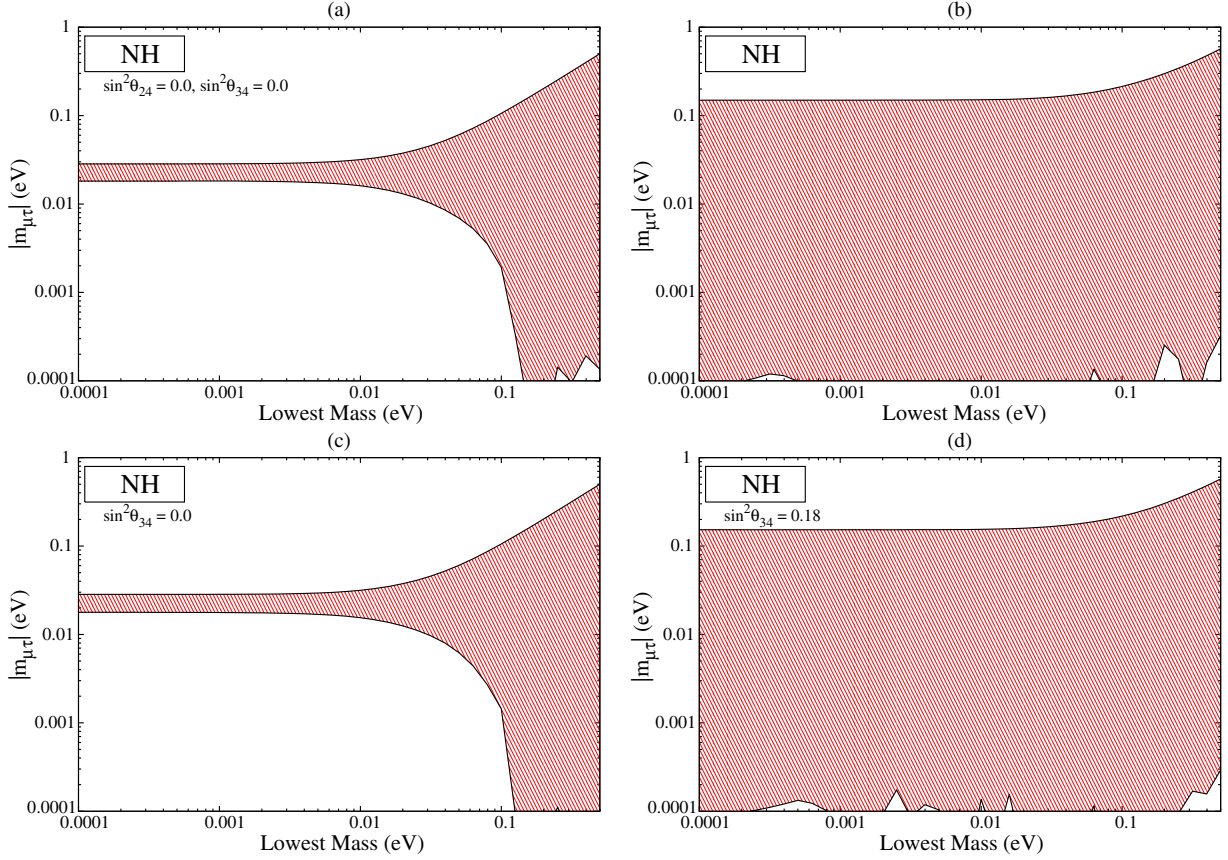


FIG. 10 (color online). Plots of vanishing $m_{\mu\tau}$ for normal hierarchy (a) for vanishing θ_{34} and θ_{24} . In panel (b) all parameters are varied in their full allowed range. Panels (c, d) are for specific values of θ_{34} when all other mixing angles are varied in their full range.

vanishing value of θ_{34} the terms with λ and λ^2 become very small and cannot cancel the leading term $\mathcal{O}(10^{-1})$. It can also be seen that in this case (i.e., $s_{34}^2 = 0$), there is no χ_{24} term in Eq. (3.31), and this is why the figure is somewhat

similar to the three-generation case. However, when θ_{34} increases these two contributions become large and cancellation becomes possible. For the case of inverted hierarchy where m_3 can have very small values, $m_{\mu\tau}$ becomes

$$\begin{aligned}
 |m_{\mu\tau}| \approx & \sqrt{\Delta m_{13}^2} \{ -c_{23}c_{34}s_{23}(c_{12}^2 e^{2i\alpha} + s_{12}^2) + \lambda[c_{12}s_{12}(1 - e^{2i\alpha})(c_{34} \cos 2\theta_{23} e^{i\delta_{13}} \chi_{13} + c_{23}s_{34} e^{i\delta_{14}} \chi_{14}) \\
 & + s_{34}\{e^{i(2\gamma+2\delta_{14}-\delta_{24})}\sqrt{\xi} - c_{23}^2 e^{i\delta_{24}}(s_{12}^2 + c_{12}^2 e^{2i\alpha})\}\chi_{24}] + \lambda^2[c_{23}c_{34}s_{23}e^{2i\delta_{13}}(c_{12}^2 + e^{2i\alpha}s_{12}^2)\chi_{13}^2 \\
 & + c_{12}s_{12}s_{23}(e^{2i\alpha} - 1)(c_{34}e^{i(\delta_{14}-\delta_{24})}\chi_{14} + 2s_{34}c_{23}e^{i(\delta_{13}+\delta_{24})}\chi_{13})\chi_{24}] \}. \quad (39)
 \end{aligned}$$

To get an idea about the magnitude of the terms, we take vanishing Majorana phases and Dirac CP phases to be of the order π . The expression in this case for vanishing $m_{\mu\tau}$ becomes

$$-c_{23}c_{34}s_{23} + \lambda(s_{34}\chi_{24}(c_{23}^2 - \sqrt{\xi})) - \lambda^2(-s_{34}\chi_{13}\chi_{14} - c_{23}c_{34}\chi_{13}^2) = 0. \quad (40)$$

In panel (a) of Fig. 11, where $|m_{\mu\tau}|$ is plotted for the three-generation case, we can see that unlike $m_{\mu\mu}$ there is no cancellation in the small m_3 region, but when plotted for the full range it gets a contribution from the sterile part and there is cancellation for the full range of m_3 [panel (b)]. Clearly, the cancellation of the terms does not become possible for small values of θ_{34} in the strict hierarchical region. This case is similar to the three-generation case in IH [cyan/light region, panel (c)]. This is because for $s_{34}^2 = 0$ the contribution of s_{24}^2 comes from the λ^2 term. If the CP violating phase α is zero, then cancellation is not possible for the whole range of m_3 [blue/dark region panel (c)]. However, as the value of s_{34}^2 increases, all the terms in the above equation become of the same order and cancellation for very small values of m_3 is possible [panel (d)].

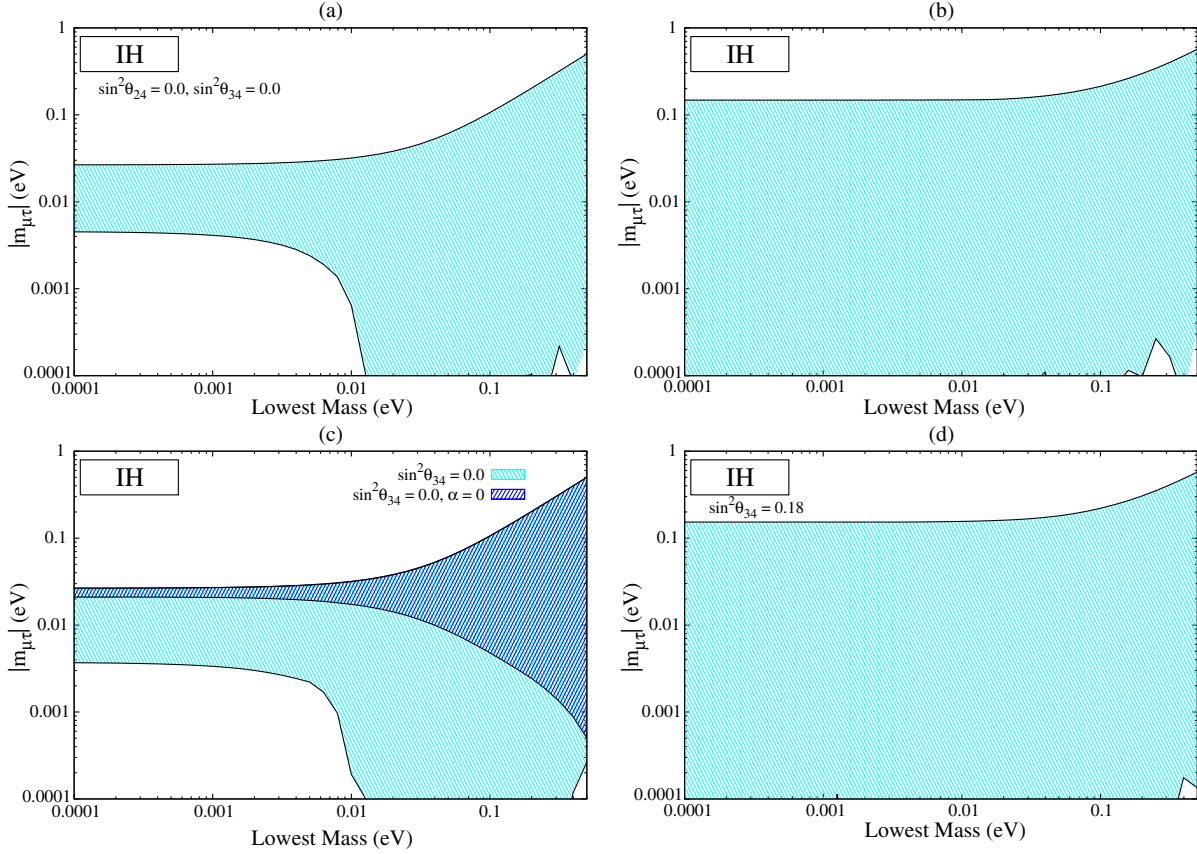


FIG. 11 (color online). Plots of vanishing $m_{\mu\tau}$ for inverted hierarchy (a) for vanishing θ_{34} and θ_{24} (three-generation case). In panel (b) all parameters are varied in their full allowed range (3 + 1). Panels (c) and (d) are for specific values of θ_{34} and α when all other mixing angles are varied in their full range.

F. The mass matrix element $m_{\tau\tau}$

This element is related to $m_{\mu\mu}$ by the $\mu - \tau$ symmetry. As discussed earlier, in the limit when θ_{24} and θ_{34} are not very large, the two mixing angles θ_{34} and θ_{24} will behave in the same way in the textures related by $\mu - \tau$ symmetry. The (3, 3) element of the neutrino mass matrix in the presence of one sterile neutrino is given as

$$\begin{aligned}
 m_{\tau\tau} = & e^{2i(\delta_{14}+\gamma)} c_{14}^2 c_{24}^2 m_4 s_{34}^2 + e^{2i(\delta_{13}+\beta)} m_3 \{ e^{i(\delta_{14}-\delta_{13})} c_{24} s_{13} s_{14} s_{34} + c_{13} (c_{23} c_{34} - e^{i\delta_{24}} s_{23} s_{24} s_{34}) \}^2 \\
 & + m_1 [-s_{12} (-c_{34} s_{23} - e^{i\delta_{24}} c_{23} s_{24} s_{34}) + c_{12} \{ -e^{i\delta_{14}} c_{13} c_{24} s_{14} s_{34} - e^{i\delta_{13}} s_{13} (c_{23} c_{34} - e^{i\delta_{24}} s_{23} s_{24} s_{34}) \}]^2 \\
 & + e^{2i\alpha} m_2 [c_{12} (-c_{34} s_{23} - e^{i\delta_{24}} c_{23} s_{24} s_{34}) + s_{12} \{ -e^{i\delta_{14}} c_{13} c_{24} s_{14} s_{34} - e^{i\delta_{13}} s_{13} (c_{23} c_{34} - e^{i\delta_{24}} s_{23} s_{24} s_{34}) \}]^2. \quad (41)
 \end{aligned}$$

This reduces to the three-generation case for $\theta_{34} = 0$. Using the approximation for normal hierarchy in Eqs. (4), (15), and (16) this becomes

$$\begin{aligned}
 |m_{\tau\tau}| \approx & \sqrt{|\Delta m_{23}^2|} \{ c_{23} c_{34} s_{23} (e^{2i\beta+\delta_{13}} - c_{12}^2 \sqrt{\xi} e^{2i\alpha}) + \lambda \{ -e^{i(2\alpha+\delta_{13})} \sqrt{\xi} s_{12} c_{12} c_{34} \cos 2\theta_{23} \chi_{13} \\
 & - \sqrt{\xi} c_{12} c_{23} s_{34} e^{2i\alpha} (s_{12} \chi_{14} e^{i\delta_{14}} + c_{12} c_{23} \chi_{24} e^{2i\delta_{24}}) + s_{34} \chi_{24} (-s_{23}^2 e^{2i(\beta+\delta_{13})+i\delta_{24}} - \sqrt{\xi} e^{2i(\gamma+\delta_{14})-i\delta_{24}}) \} \\
 & + \lambda^2 \{ \sqrt{\xi} s_{12}^2 s_{23} \chi_{13} e^{i(2\alpha+\delta_{13})} (c_{23} c_{34} \chi_{13} e^{i\delta_{13}} + s_{34} \chi_{14} e^{i\delta_{14}}) + \sqrt{\xi} c_{12} s_{12} s_{23} \chi_{24} e^{2i\alpha} (2c_{23} s_{34} \chi_{13} e^{i(\delta_{13}+\delta_{24})} \\
 & + c_{34} \chi_{14} e^{i(\delta_{14}-\delta_{24})} - s_{23} s_{34} \chi_{13} \chi_{14} e^{i(2\beta+\delta_{13}+\delta_{14})} \} \}. \quad (42)
 \end{aligned}$$

To get an idea of the order of the terms, we consider the vanishing Majorana phases and the Dirac phases having a value equal to π . This element vanishes when

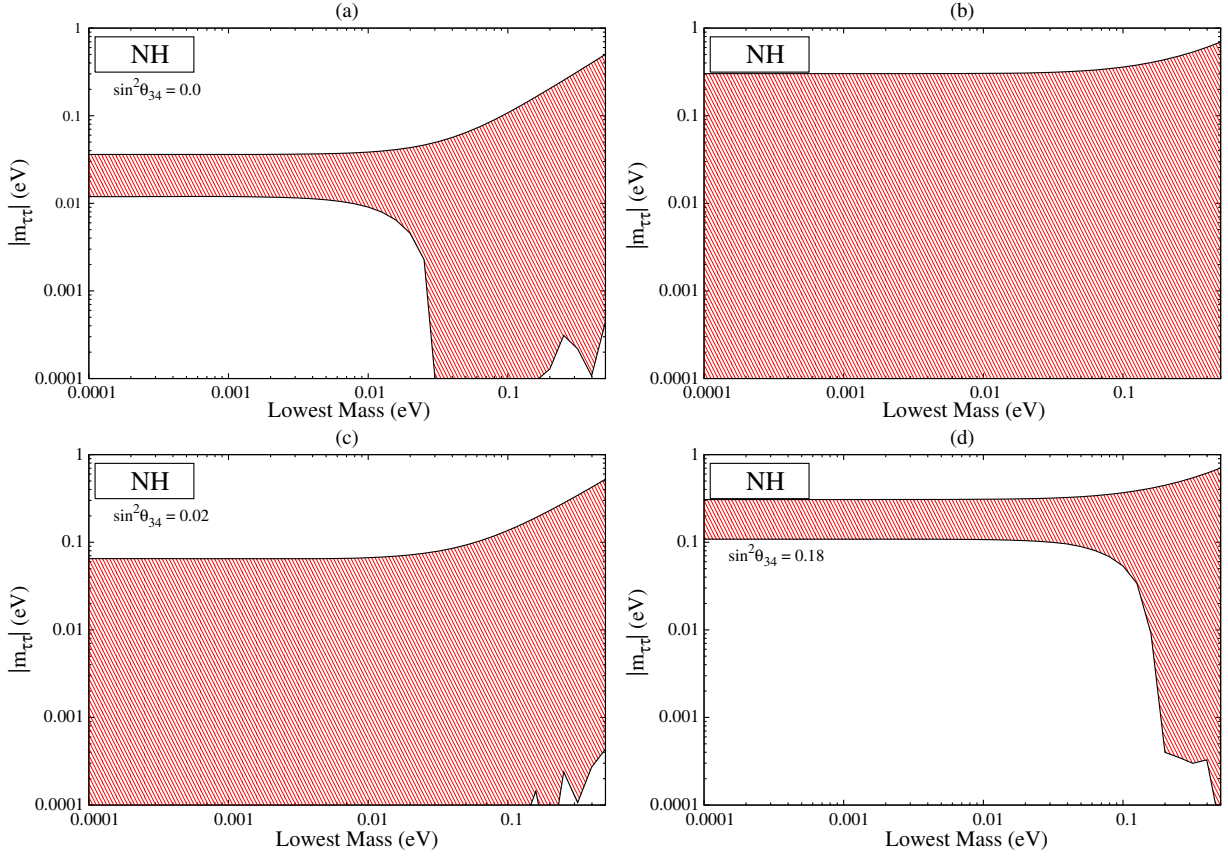


FIG. 12 (color online). Plots of vanishing $m_{\tau\tau}$ for normal hierarchy with lowest mass m_1 . Panel (a) corresponds to the three-generation case. In panel (b) all the mixing angles are varied in their full allowed range of parameters (3 + 1). Panels (c) and (d) are for some specific values of θ_{34} .

$$\begin{aligned}
 & c_{23}c_{34}s_{23}(1 - c_{12}^2\sqrt{\xi}) + \lambda\{\sqrt{\xi}s_{12}c_{12}c_{34}\cos 2\theta_{23}\chi_{13} + \sqrt{\xi}c_{12}c_{23}s_{34}(s_{12}\chi_{14} + c_{12}c_{23}\chi_{24}) - s_{34}\chi_{24}(s_{23}^2 - \sqrt{\xi})\} \\
 & + \lambda^2\{\sqrt{\xi}s_{12}^2s_{23}\chi_{13}(c_{23}c_{34}\chi_{13} + s_{34}\chi_{14}) + \sqrt{\xi}c_{12}s_{12}s_{23}\chi_{24}(2c_{23}s_{34}\chi_{13} + c_{34}\chi_{14}) + s_{23}s_{34}\chi_{13}\chi_{14}\} = 0. \quad (43)
 \end{aligned}$$

For vanishing θ_{34} , which is the case for three generations, $m_{\tau\tau} = 0$ is disallowed for small m_1 , as can be seen from panel (a) of Fig. 12. This is the generic behavior of an element belonging to the $\mu - \tau$ block in normal hierarchy which we mentioned previously. This is because for θ_{34} equal to zero the leading order term is large [$\mathcal{O}(10^{-1})$]. Here the term with λ^2 is quite small (10^{-3} – 10^{-4}) and hence will not have a very significant role to play. Thus, only terms with coefficient λ can cancel the leading order term. However, for vanishing θ_{34} this term is small, $\mathcal{O}(10^{-3})$, and cannot cancel the leading order term. In panel (b) when all the parameters are varied in their 3σ range, we can see that cancellation is possible over the whole range of m_1 (3 + 1 case). Now, when θ_{34} starts increasing from its lowest value, there exists a region for intermediate values where both the terms become approximately of the same order, and hence there can be cancellations [panel (c)]. Towards higher values of θ_{34} the term with coefficient λ becomes larger than the leading order term, due to which this mass matrix element does not vanish. For the cancellation very large values of m_1 are required, as can be seen from panel (d) of Fig. 12. For the case of inverted hierarchy, where m_3 approaches small values, we get the expression

$$\begin{aligned}
 m_{\tau\tau} \approx & c_{34}^2s_{23}^2(c_{12}^2e^{2i\alpha} + s_{12}^2) + e^{2i(\delta_{14} + \gamma)}\sqrt{\xi}s_{34}^2 + 2\lambda[(e^{2i\alpha} - 1)c_{12}c_{34}s_{12}s_{23}(c_{23}c_{34}s_{12}s_{23}(c_{23}c_{34}e^{2i\delta_{13}}\chi_{13} + e^{2i\delta_{14}}s_{34}\chi_{14}) \\
 & + 2c_{23}c_{34}e^{2i\delta_{24}}s_{23}s_{34}(c_{12}^2e^{2i\alpha} + s_{12}^2)\chi_{24}) + \lambda^2[(c_{12}^2 + e^{2i\alpha}s_{12}^2)\{c_{23}c_{34}\chi_{13}e^{i\delta_{13}}(c_{23}c_{34}\chi_{13}e^{i\delta_{13}} + 2\chi_{14}s_{34}e^{i\delta_{14}}) \\
 & + e^{2i\delta_{14}}\chi_{14}^2s_{34}^2\} + (c_{12}^2e^{2i\alpha} + s_{12}^2)c_{23}^2e^{2i\delta_{24}}\chi_{24}^2s_{34}^2 + 2s_{12}(e^{2i\alpha} - 1)e^{i\delta_{24}}(c_{34}\chi_{13}\cos 2\theta_{23}e^{i\delta_{13}} + c_{12}c_{23}\chi_{14}s_{34})s_{34}\chi_{24}]. \quad (44)
 \end{aligned}$$

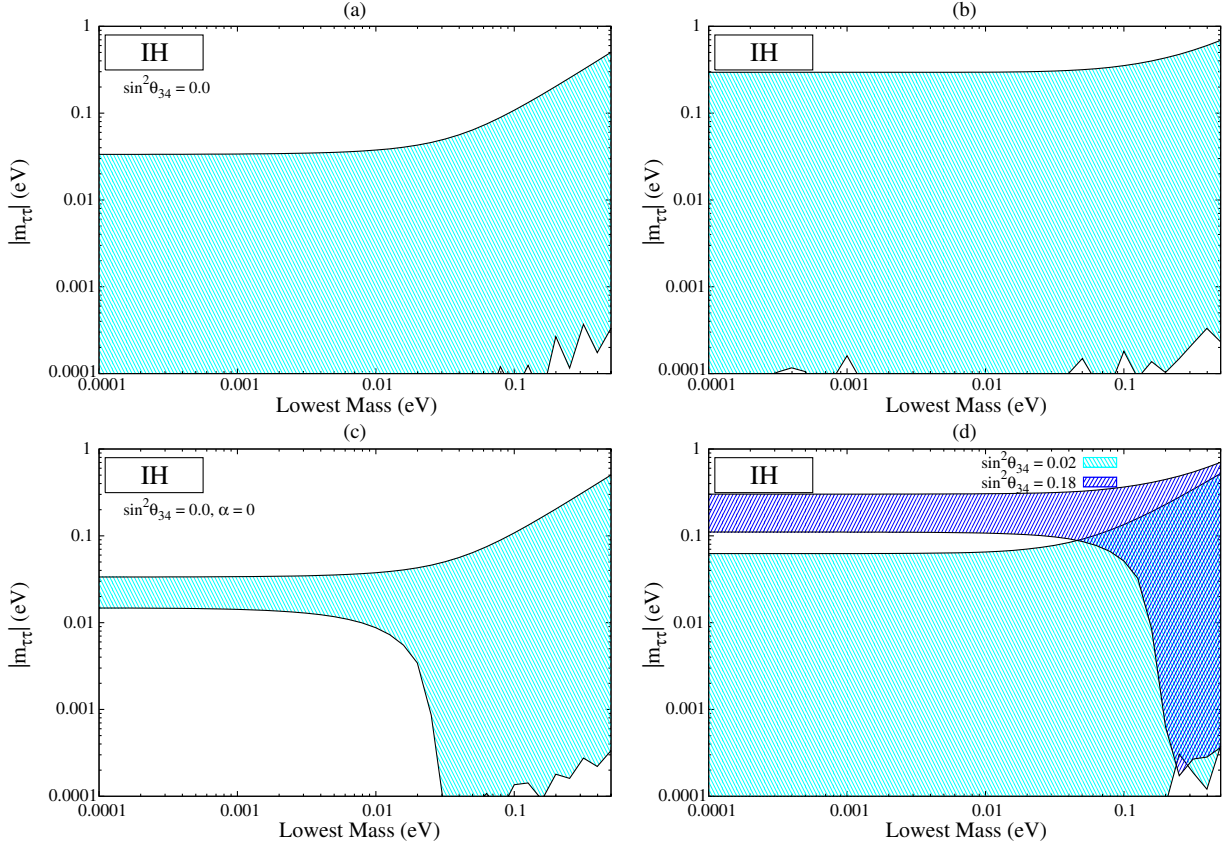


FIG. 13 (color online). Plots of vanishing $m_{\tau\tau}$ for inverted hierarchy with lowest mass m_3 . Panel (a) corresponds to the three-generation case. In panel (b) all the mixing angles are varied in their full allowed range of parameters (3 + 1). Panels (c) and (d) are for some specific values of θ_{34} and α .

For vanishing Majorana CP phases and Dirac phases having a value equal to π , this expression becomes

$$m_{\tau\tau} \approx -c_{23}c_{34}s_{23} + \lambda s_{34}\chi_{24}(c_{23}^2 - \sqrt{\xi}) + \lambda^2 s_{23}\chi_{13}(c_{23}c_{34}\chi_{13} + s_{34}\chi_{14}). \quad (45)$$

In panel (a) of Fig. 13 we reproduced the three-generation behavior by plotting $|m_{\tau\tau}|$ for $s_{34}^2 = 0$, and in panel (b) all the parameters are varied randomly (3 + 1). In both cases we can see that cancellations are possible for the whole range of m_3 . For $s_{34}^2 = 0$ all the terms are of the same order and cancellations are always possible. But if we put $\alpha = 0$, one term with coefficient λ and another term with coefficient λ^2 drop out from the equation; then small values of s_{34}^2 cannot cancel the leading order term anymore. This can

be seen from panel (c) where cancellation is not possible for the lower m_3 region. However, when s_{34}^2 increases to a value of about 0.02 this element can vanish [panel (d), the cyan region]. We see that when θ_{34} increases towards its upper bound, the λ term becomes large $\mathcal{O}(1)$. Hence, the other terms are not able to cancel this term, and we do not get a small allowed m_3 region (panel (d), blue region).

G. The mass matrix elements m_{eS} , $m_{\mu S}$, $m_{\tau S}$ and m_{SS}

The elements m_{eS} , $m_{\mu S}$, $m_{\tau S}$ and m_{SS} are present in the fourth row and fourth column in the neutrino mass matrix. They are the new elements that arise in the 3 + 1 scenario because of the addition of one light sterile neutrino. The expressions for m_{eS} and $m_{\mu S}$ are given by

$$m_{eS} = e^{i(2\gamma+\delta_{14})}c_{14}c_{24}c_{34}m_4s_{14} + e^{i(2\beta+\delta_{13})}c_{14}m_3s_{13}\{-e^{i(\delta_{14}-\delta_{13})}c_{24}c_{34}s_{13}s_{14} + c_{13}(-e^{i\delta_{14}}c_{34}s_{23}s_{24} - c_{23}s_{34})\} + c_{12}c_{13}c_{14}m_1[-s_{12}(-e^{i\delta_{24}}c_{23}c_{34}s_{24} + s_{23}s_{34}) + c_{12}\{-e^{i\delta_{14}}c_{13}c_{24}c_{34}s_{14} - e^{i\delta_{13}}s_{13}(-e^{i\delta_{24}}c_{34}s_{23}s_{24} - c_{23}s_{34})\}] + e^{2i\alpha}c_{13}c_{14}m_2s_{12}[c_{12}(-e^{i\delta_{24}}c_{23}c_{34}s_{24} + s_{23}s_{34}) + s_{12}\{-e^{i\delta_{14}}c_{13}c_{24}c_{34}s_{14} - e^{i\delta_{13}}s_{13}(-e^{i\delta_{24}}c_{34}s_{23}s_{24} - c_{23}s_{34})\}]. \quad (46)$$

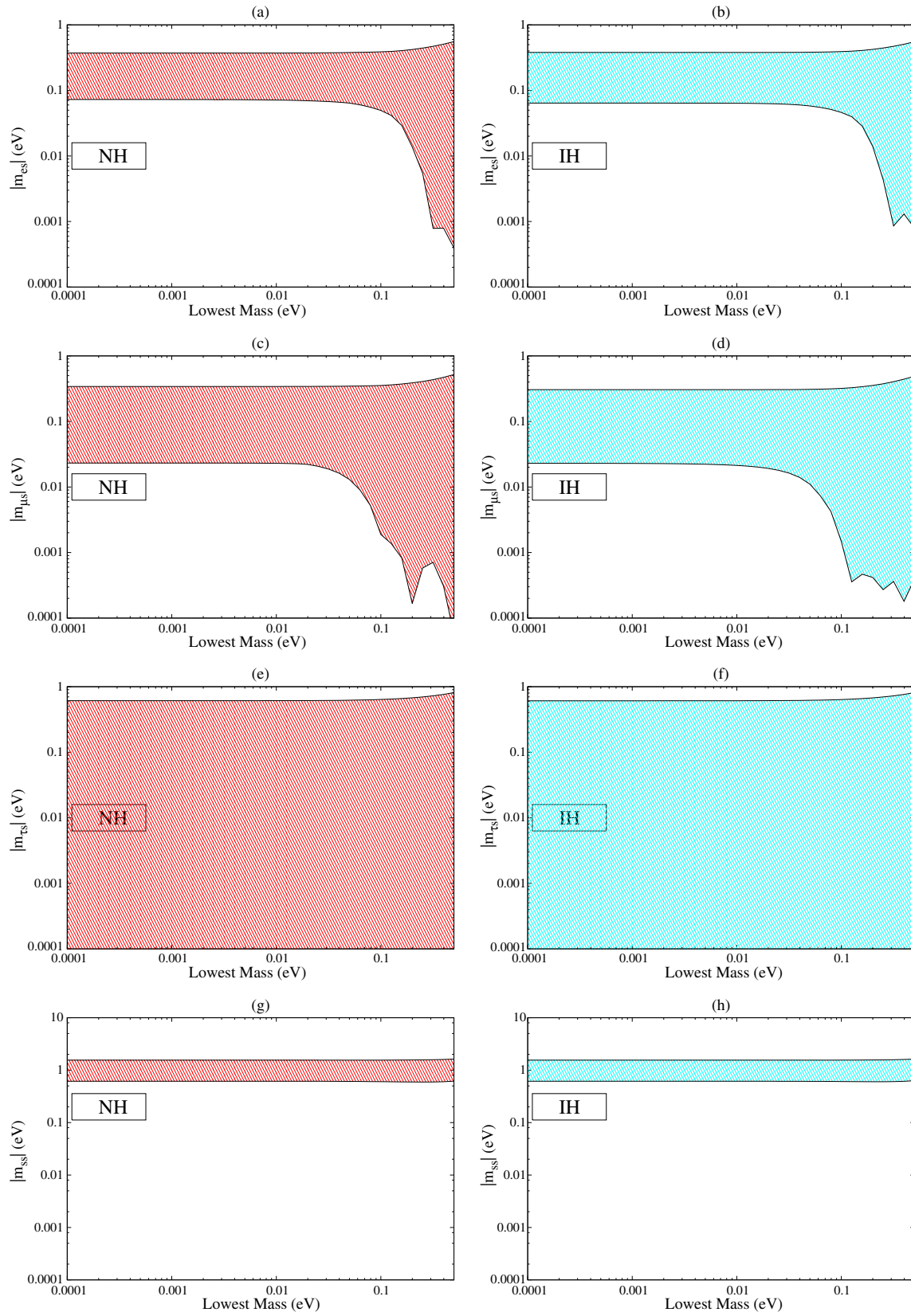


FIG. 14 (color online). Correlation plots for vanishing $|m_{k_s}|$ for both normal and inverted hierarchies. In these plots all the mixing angles are varied in their 3σ allowed range; Dirac CP phases are varied from 0 to 2π and Majorana phases from 0 to π .

$$\begin{aligned}
m_{\mu s} = & e^{i(2\gamma+\delta_{14})}c_{14}^2c_{24}c_{34}m_4s_{24} + e^{i(2\beta+\delta_{13})}m_3(c_{13}c_{24}s_{23} - e^{i(\delta_{14}-\delta_{13}-\delta_{24})}s_{13}s_{14}s_{24})\{-e^{i(\delta_{14}-\delta_{13})}c_{24}c_{34}s_{13}s_{14} \\
& + c_{13}(-e^{i\delta_{24}}c_{34}s_{23}s_{24} - c_{23}s_{34})\} + m_1\{-c_{23}c_{24}s_{12} + c_{12}(-e^{i\delta_{13}}c_{24}s_{13}s_{23} - e^{i(\delta_{14}-\delta_{24})}c_{13}s_{14}s_{24})\} \\
& \times [-s_{12}(-e^{i\delta_{24}}c_{23}c_{34}s_{24} + s_{23}s_{34}) + c_{12}\{-e^{i\delta_{14}}c_{13}c_{24}c_{34}s_{14} - e^{i\delta_{13}}s_{13}(-e^{i\delta_{24}}c_{34}s_{23}s_{24} - c_{23}s_{34})\}] \\
& + e^{2i\alpha}m_2\{c_{12}c_{23}c_{24} + s_{12}(-e^{i\delta_{13}}c_{24}s_{13}s_{23} - e^{i(\delta_{14}-\delta_{24})}c_{13}s_{14}s_{24})\} \\
& \times [c_{12}(-e^{i\delta_{24}}c_{23}c_{34}s_{24} + s_{23}s_{34}) + s_{12}\{-e^{i\delta_{14}}c_{13}c_{24}c_{34}s_{14} - e^{i\delta_{13}}s_{13}(-e^{i\delta_{24}}c_{34}s_{23}s_{24} - c_{23}s_{34})\}]. \quad (47)
\end{aligned}$$

Though the equations seem very complex, one can easily understand the properties of these elements by just looking at the m_4 terms. The m_4 term in $m_{e s}$ is proportional to s_{14} . So, in general, it is quite large [$\mathcal{O}(1)$]. For this element to become negligible, very small values of s_{14}^2 are required. But as this angle is bounded by the short baseline experiments, complete cancellations never occur for both normal and inverted hierarchies [panels (a) and (b) of Fig. 14]. Similar predictions are obtained for the $m_{\mu s}$ element, which cannot vanish since s_{24}^2 has to be negligible, which is not allowed by the data. This can be seen from panels (c) and (d) of Fig. 14.

For the element $m_{\tau s}$ the scenario is quite different.

$$\begin{aligned}
m_{\tau s} = & c_{14}^2c_{24}^2c_{34}e^{2i(\delta_{14}+\gamma)}m_4s_{34} + e^{2i(\beta+\delta_{13})}m_3\{-c_{24}c_{34}e^{i(\delta_{14}-\delta_{13})}s_{13}s_{14} + c_{13}(-c_{23}s_{34} - c_{34}e^{i\delta_{24}}s_{23}s_{24})\} \\
& \times \{-c_{24}e^{i(\delta_{14}-\delta_{13})}s_{13}s_{14}s_{34} + c_{13}(c_{23}c_{34} - e^{i\delta_{24}}s_{23}s_{34}s_{24})\} + m_1[-s_{12}(-c_{23}c_{34}e^{i\delta_{24}}s_{24} + s_{23}s_{34}) \\
& + c_{12}\{-c_{13}c_{24}c_{34}e^{i\delta_{14}}s_{14} - e^{i\delta_{13}}s_{13}(-c_{23}s_{34} - c_{34}e^{i\delta_{24}}s_{23}s_{34})\}][-s_{12}(-c_{34}s_{23} - c_{23}e^{i\delta_{24}}s_{34}s_{24}) \\
& + c_{12}\{-c_{13}c_{24}e^{i\delta_{14}}s_{14}s_{34} - e^{i\delta_{13}}s_{13}(c_{23}c_{34} - e^{i\delta_{24}}s_{23}s_{34}s_{24})\}] + e^{2i\alpha}m_2[c_{12}(-c_{23}c_{34}e^{i\delta_{24}}s_{34} + s_{23}s_{34}) \\
& + s_{12}\{-c_{13}c_{24}c_{34}e^{i\delta_{14}}s_{14} - e^{i\delta_{13}}s_{13}(-c_{23}s_{34} - c_{34}e^{i\delta_{24}}s_{23}s_{24})\}][c_{12}(-c_{34}s_{23} - c_{23}e^{i\delta_{24}}s_{34}s_{24}) \\
& + s_{12}\{-c_{13}c_{24}e^{i\delta_{14}}s_{14}s_{34} - e^{i\delta_{13}}s_{13}(c_{23}c_{34} - e^{i\delta_{24}}s_{23}s_{34}s_{14})\}]. \quad (48)
\end{aligned}$$

In this case the m_4 term is proportional to θ_{34} and there is no lower bound on it from the short baseline experiments; i.e., it can approach smaller values. As a result the term with m_4 can be very small. Thus this matrix element can possibly vanish in both hierarchies for the whole range of the lowest mass [panels (e) and (f)].

The (4, 4) element of the neutrino mass matrix is given as

$$\begin{aligned}
m_{ss} = & c_{14}^2c_{24}^2c_{34}^2e^{2i(\gamma+\delta_{14})}m_4 + e^{2i(\beta+\delta_{13})}m_3\{-c_{24}c_{34}e^{i(\delta_{14}-\delta_{13})}s_{13}s_{14} + c_{13}(-c_{23}s_{34} - c_{34}e^{i\delta_{24}}s_{23}s_{24})\}^2 \\
& + m_1[-s_{12}(-c_{23}c_{34}e^{i\delta_{24}}s_{24} + s_{23}s_{34}) + c_{12}\{-c_{13}c_{24}c_{34}e^{i\delta_{14}}s_{14} - e^{i\delta_{13}}s_{13}(-c_{23}s_{34} - c_{34}e^{i\delta_{24}}s_{23}s_{24})\}]^2 \\
& + e^{2i\alpha}m_2[c_{12}(-c_{23}c_{34}e^{i\delta_{24}}s_{24} + s_{23}s_{34}) + s_{12}\{-c_{13}c_{24}c_{34}e^{i\delta_{14}}s_{14} - e^{i\delta_{13}}s_{13}(-c_{23}s_{34} - c_{34}e^{i\delta_{24}}s_{23}s_{34})\}]^2. \quad (49)
\end{aligned}$$

The m_4 term for m_{ss} is proportional to $c_{14}^2c_{24}^2c_{34}^2$. One can see that this term is of order one; as a result, this element can never vanish, as is evident from panels (g) and (h).

IV. CONCLUSIONS

In this paper we analyze systematically the one-zero textures of the 4×4 mass matrix in the presence of a sterile neutrino. Assuming neutrinos to be Majorana particles, this is a symmetric matrix with 10 independent entries. We use the information on the active sterile mixing angles from the short baseline experiments. We analyze if the current constraints on oscillation parameters allow each of these entries to assume a vanishing value. We also study the implications and correlations among the parameters when each matrix element is zero. We expand the mass matrix element in terms of a parameter λ with suitable coefficients χ_{13} , χ_{14} and χ_{24} corresponding to the mixing angles θ_{13} , θ_{14} and θ_{24} . This is motivated by the

observation that these angles are of the same order with $\lambda \equiv 0.2$. These expressions facilitate the analytic understanding of the numerical results presented in the different plots. We study the vanishing condition as a function of the lowest mass m_1 (NH) or m_3 (IH) by varying the lightest mass in the range 0.0001–0.5 eV.

We find that $|m_{ee}| = 0$ is possible for NH only for higher values of the smallest mass m_1 , while for IH it is possible even for lower values. This is in sharp contrast to the three-generation case, where complete cancellation can never take place for IH. The current and upcoming $0\nu\beta\beta$ experiments like GERDA, CUORE, MAJORANA, EXO, SuperNEMO, KamLAND-ZEN, and SNO+ [28–30] can lower the present sensitivity by 1 order of magnitude (~ 0.012 – 0.06 eV) and hence can probe the IH region for the three-neutrino scheme [31]. However, for the $3 + 1$ scenario, m_{ee} can be in the range of the expected sensitivity of the future $0\nu\beta\beta$ experiments, even for NH. Thus if the existence of sterile neutrinos is confirmed by

future experiments [32], then it may be difficult to probe the hierarchy from $0\nu\beta\beta$ alone.

$|m_{e\mu}|$ can vanish over the whole range of the smallest mass for both three- and 3 + 1-neutrino scenarios. However, for larger values of the mixing angle s_{24}^2 , cancellation is not achieved for smaller m_1 for NH. For IH the cancellation condition depends on the Majorana phase α and the mixing angle θ_{24} . We obtain the correlations between these two parameters, which is required for making this element vanishingly small.

Cancellation is achieved for the element $m_{e\tau}$ for the full range of the lowest mass in the 3 + 1 scenario. The element $m_{e\mu}$ is related to the element $m_{e\tau}$ by $\mu - \tau$ symmetry. However, unlike the three-generation case, θ_{23} in these textures are not related simply by $\bar{\theta}_{23} = (\pi/2 - \theta_{23})$. The mixing angles θ_{24} and θ_{34} are also different in these two textures, in general. However, for small values of θ_{24} we get $\bar{\theta}_{24} = \theta_{34}$ in these textures. Consequently, the role played by θ_{24} for $m_{e\mu}$ is played by θ_{34} in $m_{e\tau}$ in this limit. Thus, in this case cancellation is not achieved for larger values of s_{34}^2 in the hierarchical regime for NH. For IH we obtain correlations between α and $\sin^2\theta_{34}$ for fulfilling the condition for cancellations.

The elements $m_{\mu\mu}$ and $m_{\tau\tau}$ are related by $\mu - \tau$ symmetry. For these cases, cancellation is not possible in the hierarchical zone for IH, in the three-generation case. However, the extra contribution coming from the sterile part helps in achieving cancellation in this region. For IH

one can obtain correlations between the Majorana phase α and the mixing angle $\theta_{24}(\theta_{34})$ for $|m_{\mu\mu}| = 0(|m_{\tau\tau}| = 0)$.

For $m_{\mu\tau}$ element cancellation was possible for the three-generation case only for higher values of the lightest mass. However, if one includes the sterile neutrino then this element can vanish over the whole range of the lightest neutrino mass considered.

With the current constraints on sterile parameters it is not possible to obtain $m_{ss} = 0$, while m_{es} and $m_{\mu s}$ can only vanish in the QD regime of the active neutrinos. However, the element $m_{\tau s}$ can be vanishingly small in the whole mass range. This is because the angle θ_{34} can take very small values, and hence cancellation is possible even for smaller values of the lowest mass.

The above results can be useful for building models for light sterile neutrinos and can shed light on the underlying new physics if future experiments and analyses reconfirm the explanation of the present anomalies in terms of sterile neutrinos.

ACKNOWLEDGMENTS

The work of C.S.K. and S.G. is supported by the National Research Foundation of Korea (NRF) through a grant funded by the Korean government of the Ministry of Education, Science and Technology (MEST) (Grants No. 2011-0017430 and No. 2011-0020333).

-
- [1] C. Athanassopoulos *et al.* (LSND Collaboration), *Phys. Rev. Lett.* **77**, 3082 (1996); **81**, 1774 (1998); A. Aguilar-Arevalo *et al.* (LSND Collaboration), *Phys. Rev. D* **64**, 112007 (2001).
 - [2] J. J. Gomez-Cadenas and M. C. Gonzalez-Garcia, *Z. Phys. C* **71**, 443 (1996); S. Goswami, *Phys. Rev. D* **55**, 2931 (1997); N. Okada and O. Yasuda, *Int. J. Mod. Phys. A* **12**, 3669 (1997); V. D. Barger, T. J. Weiler, and K. Whisnant, *Phys. Lett. B* **427**, 97 (1998).
 - [3] M. Maltoni, T. Schwetz, M. A. Tortola, and J. W. F. Valle, *Phys. Rev. D* **67**, 013011 (2003).
 - [4] A. A. Aguilar-Arevalo *et al.* (MiniBooNE Collaboration), *Phys. Rev. Lett.* **110**, 161801 (2013); **103**, 061802 (2009).
 - [5] C. Giunti and M. Laveder, *Phys. Lett. B* **706**, 200 (2011); C. Giunti, M. Laveder, Y. F. Li, Q. Y. Liu, and H. W. Long, *Phys. Rev. D* **86**, 113014 (2012).
 - [6] J. Kopp, M. Maltoni, and T. Schwetz, *Phys. Rev. Lett.* **107**, 091801 (2011); J. M. Conrad, C. M. Ignarra, G. Karagiorgi, M. H. Shaevitz, and J. Spitz, *Adv. High Energy Phys.* **2013**, 163897 (2013).
 - [7] C. Giunti and M. Laveder, *Phys. Rev. D* **84**, 073008 (2011).
 - [8] G. Mention, M. Fechner, Th. Lasserre, Th. A. Mueller, D. Lhuillier, M. Cribier, and A. Letourneau, *Phys. Rev. D* **83**, 073006 (2011).
 - [9] C. Giunti and M. Laveder, *Phys. Rev. C* **83**, 065504 (2011).
 - [10] Z. Hou, R. Keisler, L. Knox, M. Millea, and C. Reichardt, *Phys. Rev. D* **87**, 083008 (2013).
 - [11] P. A. R. Ade *et al.* (Planck Collaboration), [arXiv:1303.5076](https://arxiv.org/abs/1303.5076).
 - [12] A. Mirizzi, G. Mangano, N. Saviano, E. Borriello, C. Giunti, G. Miele, and O. Pisanti, [arXiv:1303.5368](https://arxiv.org/abs/1303.5368).
 - [13] K. N. Abazajian, M. A. Acero, S. K. Agarwalla, A. A. Aguilar-Arevalo, C. H. Albright, S. Antusch, C. A. Argüelles, A. B. Balantekin *et al.*, [arXiv:1204.5379](https://arxiv.org/abs/1204.5379).
 - [14] P. Minkowski, *Phys. Lett.* **67B**, 421 (1977); T. Yanagida, in Workshop on Unified Theories, KEK Report No. 79-18, 1979, p. 95; M. Gell-Mann, P. Ramond, and R. Slansky, *Supergravity* (North Holland, Amsterdam, 1979), p. 315; R. N. Mohapatra and G. Senjanovic, *Phys. Rev. Lett.* **44**, 912 (1980).
 - [15] S. K. Kang and C. S. Kim, *Phys. Rev. D* **63**, 113010 (2001); P. H. Frampton, S. L. Glashow, and D. Marfatia, *Phys. Lett. B* **536**, 79 (2002).

- [16] S. Dev, S. Kumar, S. Verma, and S. Gupta, *Phys. Rev. D* **76**, 013002 (2007); Z.Z. Xing, *Phys. Lett. B* **530**, 159 (2002); **539**, 85 (2002); B.R. Desai, D.P. Roy, and A.R. Vaucher, *Mod. Phys. Lett. A* **18**, 1355 (2003); S. Dev, S. Kumar, S. Verma, and S. Gupta, *Phys. Lett. B* **656**, 79 (2007); *Nucl. Phys.* **B784**, 103 (2007); S. Kumar, *Phys. Rev. D* **84**, 077301 (2011); H. Fritzsch, Z.-z. Xing and S. Zhou, *J. High Energy Phys.* **09** (2011) 083; D. Meloni and G. Blankenburg, *Nucl. Phys.* **B867**, 749 (2013); P.O. Ludl, S. Morisi, and E. Peinado, *Nucl. Phys.* **B857**, 411 (2012); W. Grimus and P.O. Ludl, *J. Phys. G* **40**, 055003 (2013).
- [17] M. Ghosh, S. Goswami, and S. Gupta, *J. High Energy Phys.* **04** (2013) 103.
- [18] Y. Zhang, *Phys. Rev. D* **87**, 053020 (2013).
- [19] A. Merle and W. Rodejohann, *Phys. Rev. D* **73**, 073012 (2006).
- [20] E.I. Lashin and N. Chamoun, *Phys. Rev. D* **85**, 113011 (2012).
- [21] S. Goswami and W. Rodejohann, *Phys. Rev. D* **73**, 113003 (2006).
- [22] G.L. Fogli, E. Lisi, A. Marrone, D. Montanino, A. Palazzo, and A.M. Rotunno, *Phys. Rev. D* **86**, 013012 (2012).
- [23] M. Archidiacono, N. Fornengo, C. Giunti, and A. Melchiorri, *Phys. Rev. D* **86**, 065028 (2012).
- [24] T. Schwetz, in *Proceedings of Sterile Neutrinos at Crossroads* (Virginia Tech, USA, 2011).
- [25] M.C. Gonzalez-Garcia, M. Maltoni, J. Salvado, and T. Schwetz, *J. High Energy Phys.* **12** (2012) 123.
- [26] D.V. Forero, M. Tortola, and J.W.F. Valle, *Phys. Rev. D* **86**, 073012 (2012).
- [27] J. Barry, W. Rodejohann, and H. Zhang, *J. High Energy Phys.* **07** (2011) 091.
- [28] A. Gando *et al.* (KamLAND-Zen Collaboration), *Phys. Rev. Lett.* **110**, 062502 (2013).
- [29] M. Auger *et al.* (EXO Collaboration), *Phys. Rev. Lett.* **109**, 032505 (2012).
- [30] <http://www.mpi-hd.mpg.de/gerda/>; P. Gorla (CUORE Collaboration), *J. Phys. Conf. Ser.* **375**, 042013 (2012); J.F. Wilkerson *et al.* (MAJORANA Collaboration), *J. Phys. Conf. Ser.* **375**, 042010 (2012); A. Barabash *et al.* (SuperNEMO Collaboration), *J. Phys. Conf. Ser.* **375**, 042012 (2012); J. Hartnell (SNO+ Collaboration), *J. Phys. Conf. Ser.* **375**, 042015 (2012).
- [31] For a recent compilation of the sensitivity limits of the future experiments, see for instance W. Rodejohann, *J. Phys. G* **39**, 124008 (2012).
- [32] A. Esmaili and A. Y. Smirnov, [arXiv:1307.6824](https://arxiv.org/abs/1307.6824).